UNIVERSITY OF CAPE TOWN

FACULTY OF SCIENCE

DEPARTMENT OF OCEANOGRAPHY

A MODEL STUDY OF THE INTERANNUAL VARIABILITY OF TANZANIAN RAINFALL

BY

SAIGURAN LOISULIE

SUPERVISOR: PROF. REASON, C. J. C

MINI-DISSERTATION SUBMITTED TO THE FACULTY OF SCIENCE AS A REQUIREMENT FOR THE PARTIAL FULFILMENT OF THE MASTER OF SCIENCE DEGREE IN APPLIED MARINE SCIENCE (OCEANOGRAPHY)

November 2006

Abstract

The ability of the Hadley Centre Atmospheric Model version 3 (HadAM3) to capture rainfall variability patterns over Eastern Africa and the western tropical Indian Ocean during the rainy seasons (October to December (OND) and March to May (MAM)) is assessed against data derived from National Centre for Environmental Prediction (NCEP) model and Global Precipitation Climatology Project (GPCP). The vector winds climatology at 850hPa and 200hPa reveals some comparable patterns in both HadAM3 and NCEP. However, there are indications that the Somali Jet appears earlier and the monsoon easterly winds over the western Indian Ocean are weaker in HadAM3 than in NCEP. Empirical Orthogonal Functions (EOF) and Principal Component Analysis (PCA) derived from the GPCP precipitation, and NCEP Outgoing Longwave Radiation (OLR) and geopotential anomalies were also compared to those from the HadAM3 model. An obvious difference was revealed between the OND and MAM rainy seasons in the ability of the HadAM3 model to capture the spatiotemporal patterns of variability displayed in both GPCP and NCEP models. The leading EOFs of precipitation anomalies patterns indicate that the performance of HadAM3 in capturing the patterns shown in GPCP data during the OND season is considerably better than that in MAM. Sea Surface Temperature Anomalies (SSTAs) over the western tropical Indian Ocean have been indicated to have a significant influence on the OND season but little on MAM. It is therefore concluded that the lesser success of the HadAM3 model for MAM may be attributed to the fact that its monsoon easterlies are too weak over the western tropical Indian Ocean causing the model to capture less rainfall over East Africa. Using regional atmospheric models with improved monsoon winds which are indicated to have a strong impact on the MAM season rains as a boundary condition may improve the simulation of precipitation in this season.

Acknowledgements

Full funding from the Nairobi based African Network of Scientific and Technological Institutions (ANSTI) is gratefully acknowledged. Thanks are also extended to NCEP, GPCP and CRU for granting a free access to their datasets. Supervision from Professor Chris Reason of the University of Cape Town – Department of Oceanography is highly appreciated. Special appreciations are owed to K Hansingo, a PhD student in the Department of Oceanography for assisting with the analysis of some data and preparation of some diagrams.

TABLE OF CONTENTS

ABSTRACT I

ACKNOWLEDGEMENTS II

DECLARATION III

1.0 INTRODUCTION 1

1.1 STUDY OBJECTIVES 1

1.2 LITERATURE REVIEW 1

1.3 REPORT ORGANIZATION 7

2 MODEL DESCRIPTION, DATA AND METHODOLOGY 7

3 RESULTS 13

3.1 MONTHLY RAINFALL CLIMATOLOGY 14

3.2 INTERANNUAL RAINFALL VARIABILITY 17

3.3 COMPARISON OF HADAM3 AND NCEP VECTOR WINDS CLIMATOLOGY DURING OND AND MAM 22

3.4 EMPIRICAL ORTHOGONAL FUNCTIONS (EOFS) AND PRINCIPAL COMPONENT ANALYSIS (PCA) 27

4 DISCUSSION 38

5 CONCLUSIONS AND RECOMMENDATIONS 40

REFERENCES 41

APPENDIX: SECOND AND THIRD EOF/PCA FIGURES 47

LIST OF FIGURE

Fig. 1. The map of Tanzania showing rainfall stations used in this study 11
Fig. 2. The 1985-2003 monthly climatology of station rainfall in *mm/month* over different areas of Tanzania, the station names are: a) Dar es Salaam, b) Arusha, c) Bukoba, d) Dodoma, e) Kigoma, f) Mbeya and g) Mtwara. 16
Fig. 3. GPCP and HadAM3 model precipitation climatology in *mm/day* for MAM and OND seasons 17
Fig. 4. Standardized departures of interannual station rainfall variability over Tanzania, the figure shows on the top left variability during the MAM season, top right variability during the OND season, bottom left El Nino years and bottom right La Nina years. (Note that the vertical scales in each panel are different)... 19
Fig. 5. The comparison of precipitation anomalies derived from GPCP and HadAM3 model for OND 1997 19
Fig. 6. Interannual timeseries of CRU 2.1 TS rainfall in *mm/month* during MAM and OND season with a ten year moving average. (Note that the vertical scales in each panel are different) 20
Fig. 7. Departures of CRU 2.1 TS decadal rainfall variability in *mm/month* over Tanzania (0 to 12S and 30E to 41E) during MAM and OND seasons. (Note that the vertical scales in each panel are different). 21
Fig. 8. HadAM3 and NCEP 850hPa vector winds climatology and their difference for MAM 23
Fig. 9. HadAM3 and NCEP 200hPa vector winds climatology and their difference for MAM 24
Fig. 10. HadAM3 and NCEP 850hPa vector winds climatology and their difference for OND 25
Fig. 11. HadAM3 and NCEP 200hPa vector winds climatology and their difference for OND 26
Fig. 12. The GPCP and HadAM3 model OND precipitation anomalies first EOF with variance contribution of 38% and 56% respectively, the positive EOFs are shaded. 30
Fig. 13. Interannual variability of precipitation anomalies first PCA derived from GPCP and HadAM3 model for OND season 30
Fig. 14. The NCEP and HadAM3 model OND OLR first EOF with variance contribution of 32% and 66% respectively, the positive EOFs are shaded. 31
Fig. 15. Temporal patterns of NCEP and HadAM3 model OLR anomalies PCA for the OND season. 31
Fig. 16. The NCEP and HadAM3 model OND 850hPa geopotential height first EOF with variance contribution of 71% and 81% respectively the positive EOFs are shaded 32
Fig. 17. Temporal patterns of NCEP and HadAM3 model 850hPa geopotential height anomalies PCA for the OND season 32
Fig. 18. The NCEP and HadAM3 model OND 200hPa geopotential height first EOF with variance contribution of 84% and 90% respectively, positive EOFs are shaded. 33
Fig. 19. Temporal patterns of NCEP and HadAM3 model 200hPa geopotential height anomalies first PCA for the OND season. 33
Fig. 20. The GPCP and HadAM3 model MAM precipitation anomalies first EOF with

variance contribution of 31% and 33% respectively, positive EOFs are shaded. 34
Fig. 21. Temporal patterns of GPCP and HadAM3 model precipitation anomalies first PCA for the MAM season. 34
Fig. 22. The NCEP and HadAM3 model MAM OLR anomalies first EOF with variance contribution of 23% and 46% respectively, positive EOF are shaded. 35
Fig. 23. Temporal patterns of NCEP and HadAM3 OLR anomalies first PCA for the MAM season 35
Fig. 24. The NCEP and HadAM3 model MAM 850hPa geopotential height anomalies first EOF with variance contribution of 74% and 60% respectively, positive EOF are shaded. . 36
Fig. 25. Temporal patterns of NCEP and HadAM3 850hPa geopotential height anomalies first PCA for the MAM season. 36
Fig. 26. The NCEP and HadAM3 model MAM 200hPa geopotential height anomalies first EOF with variance contribution of 94% and 93% respectively 37
Fig. 27. Temporal patterns of NCEP and HadAM3 200hPa geopotential height anomalies first PCA for the MAM season. 37

1.0 Introduction

Tanzania depends on rainfall as the major source of water for domestic, agricultural and industrial uses. For this reason, the availability of reliable information on the anticipated amount and distribution of rainfall is of great significance in the management of water resources. The ongoing rationing of electricity in the country due to lack of enough water in the dams may be taken as a prominent example indicating the importance of rainfall variability information in the management of water resources. The occurrence of unprecedented extreme weather events like droughts and floods is a great challenge for agricultural and industrial planning. Given the fact that the amount and distribution of rainfall over the country are very variable and difficult to predict, these problems may remain unchecked until a proper solution is brought forward by the scientific community. An investigation into reliable and valid tools, like ocean and atmospheric circulation models for climate prediction and weather forecasting needs therefore to be considered for possible solutions of the current problem.

1.1 Study Objectives

Therefore, this study aims at investigating the observational and model simulated spatial and temporal variability of rainfall over Tanzania from 1985 to 2003 at a seasonal to an interannual time scale. The objective is to assess the ability of the Hadley Centre Atmospheric Model version 3 (HadAM3) (Pope et al., 2000) to capture and display seasonal and interannual features identified in the National Centre for Environmental Prediction (NCEP) model (Kalnay et al., 1996; www.cdc.noaa.gov), Global Precipitation Climatology Project (GPCP) (Adler et al., 2003; http://cics.umd.edu/~yin/GPCP), Tanzania Meteorological Agency (TMA) and Climate Research Unit (CRU) (Mitchell and Philip, 2005) data. To achieve this objective, a clear understanding of temporal and spatial rainfall variability over Tanzania is needed. This has been established to some extent through meteorological studies done over the country and eastern Africa.

1.2 Literature Review

There are two rainfall seasons over Tanzania which are determined by their relative position to the meridional movement of the Intertropical Convergence Zone (ITCZ) and the associated northeast and southeast trade winds (Alusa and Gwange, 1978; Mhita and Nassib, 1987; Mhita, 2003). These rainfall seasons are called the unimodal and bimodal. The unimodal rains, which are experienced over southern and western Tanzania, are characterized by one long uninterrupted rainfall season from November to April which comes as the ITCZ moves further into the Southern Hemisphere in austral summer and moves north of the equator in March. The bimodal regions show two distinctive rainfall seasons, one is commonly known as short rains (vuli) which occurs from October to December (OND), during the southward journey of the ITCZ and the other is the long rains (masika) which begins in March and recedes in May (MAM) and coincides with the northward shift of the ITCZ (Mutai and Ward, 2000; Kijazi and Reason, 2005). Bimodal rains are experienced over northern and eastern Tanzania. Mhita (2003) gives a further categorization of the above two modes of rainfall into ten zones of homogeneous rainfall.

However, in some areas near Lake Victoria and the Indian Ocean, rainfall may be recorded at any time of the year (Asnani, 1993). Moreover, it has also been reported that there are peculiar rainfall patterns over the areas under the immediate influence of orographic features (Asnani, 1993).

Relative to the long rains, the short rains tend to have stronger interannual variability (Kabanda and Jury, 1999 and 2000), stronger spatial coherence of rainfall anomalies, and substantial association with El Niño-Southern Oscillation (ENSO) and Sea Surface Temperature (SST) patterns (Ropelewski and Halpert 1987, 1996; Ogallo and Suleiman., 1988; Beltrando 1990; Hastenrath et al., 1993; Nicholson and Kim 1997; Mutai and Ward 2000; Reason et al., 2000; Kijazi and Reason, 2005; Mapande and Reason, 2005). These studies described that warm events of ENSO tend to be associated with above average rainfall during OND. The existence of intraseasonal rainfall variability has also been demonstrated (Mpeta, 1997; Mapande and Reason, 2005)

It was stated earlier that Tanzanian rainfall seasonality and variability are influenced by the passage of the ITCZ, and the associated trade winds (northeasterlies and southeasterlies), which move relative to the position of the overhead sun. These winds are also known as monsoon winds (Okoola, 1999). The relationship between ITCZ movement and Tanzania rainfall seasonality is described by Asnani (1993). Also, interannual climate variability over Tanzania may be caused by ENSO, Quasi-biennial Oscillation (QBO), Indian Ocean Dipole/Zonal Mode (Ogallo et al., 1988; Ogallo, 1988 and 1989; Nicholson, 1996; Saji et al., 1999; Webster et al., 1999; Indeje and Semazzi, 2000, Reason et al., 2000). In addition, mesoscale systems generated by orography, large inland lakes and other surface contrasts have also been shown to contribute significantly to the diurnal, seasonal and even interannual climate variability over the country (Datta, 1981; Asnani, 1993; Mukabana and Pielke, 1996; Sun et al., 1999a&b).

The East African monsoon has a significant influence on Tanzania rainfall variability and its association with the position of the ITCZ is suggested as a reason for this influence (Nyenzi, 1988; Mutai and Ward, 1998; Asnani, 1993, Okoola, 1999).

In October, the ITCZ moves southward from about 2^{o}S to about 12^{o}S by the end of December. It remains in this extreme southern position up to about the end of January and then slowly starts on its northward return journey and by the end of April it is located near 2^{o}S. As the ITCZ moves first southwards and then northwards, the rains also move with it. On its southward journey, the ITCZ causes rains over some areas of Tanzania from mid-October to mid-December. This period is locally called the season of "Short Rain". These areas again get rains from about middle of March to the beginning of June with northward journey of the ITCZ, locally called the season of "Long Rains". South, West and Central Tanzania gets rains from November to April.

During the period of "Short Rains", northeasterlies and northerlies replace the southeasterlies in the lower tropcsphere along the coast of Tanzania, in association with the build up of the anticyclonic ridge over Arabia. For the period of "Long Rains", low level southeasterlies strengthen along the coast of Tanzania until the Somali Jet is established over the coast of East Africa by the end of June. However, the determination of the fixed dates for the onset and withdrawal of Monsoon in East Africa has proved to be an outstanding challenge (Alusa and Mushi 1974; Alusa 1978).

Investigations over the Indian Ocean suggest the presence of ENSO related warming in this ocean (Toure and White, 1997; Chambers et al., 1999; Reason et al., 2000). Furthermore, other investigations have shown that ENSO is a predominant factor responsible in modulating rainfall variability over East Africa (Ropelewski and Halpert, 1987, Janowiak, 1988; Ogallo 1988; Hastenrath et al., 1993; Hutchison, 1992; Nicholson and Kim, 1997; Indeje et al., 2000; Mutai and Ward, 2000; Amissah-Arthur et al., 2002; Mistry and Conway 2003, Kijazi and Reason 2005). As cited previously, the short rains tend to have a strong relationship with ENSO. Short rains during OND over East Africa shows a relationship with the strength of the equatorial surface westerlies over the Indian Ocean and the zonal pressure gradient across the basin, and both of these variables are modulated during ENSO (Hastenrath and Polzin, 2004). ENSO predominantly affects the long term variability of rainfall over Lake Victoria, which is a crucial source of water and food to East and Northeast Africa (Mistry and Conway, 2003). This is revealed from the Lake Victoria Rainfall Series (LVRS) and OND and MAM Empirical Orthogonal Functions (EOF) series analysis.

Furthermore, it has been observed that during El Niño (La Niña) events, typical rainfall tends to be enhanced (reduced) over equatorial East Africa (Camberlin, 1995; Nicholson, 1996; Kijazi and Reason, 2005). Above (below) average rainfall over northern Tanzania coast during OND and to a lesser extent during MAM appears to be associated with El Niño (La Niña) but ENSO impacts were reported to be less coherent over the southern coast of Tanzania (Kijazi and Reason, 2005). Moreover, a longer (shorter) than average rainfall season associated with early (late) onset is a contributing factor to the increased (reduced) rainfall occurring over the north (south) coast of Tanzania during El Niño years (Kijazi and Reason, 2005).

The QBO, which is a quasi-periodic reversal in the tropospheric and stratospheric zonal wind from easterly to westerly components and vice versa with a periodicity of about 28 months, has been exhibited by African rainfall (Rodhe and Virji, 1976; Ogallo, 1982; Nicholson and Entekhabi, 1986; Nicholson, 1996). Indeje and Semazzi (2000) revealed that there is a correlation between QBO and East African seasonal rainfall and that the relationship is stronger during June-August and weakest during December-February. Furthermore, it is strongly phase locked with annual cycle and it also tends to enhance major negative swings in Southern Oscillation (SO) associated with the ENSO events (Indeje and Semazzi, 2000). The development of ENSO seems to be associated with the easterly phase of the lower stratospheric QBO (Lau and Sheu, 1988).

The Indian Ocean Dipole Mode (IODM), which is characterized by warm Sea Surface Temperature Anomalies (SSTAs) and cold SSTAs in the western and tropical eastern Indian Ocean in its positive phase respectively, has been shown to influence northern Tanzanian rainfall variability (Saji et al., 1999; Webster et al., 1999). This was suggested after discovering that the anomalous conditions that occurred in the Indian Ocean during certain years may be independent of ENSO. During the positive phase of the mode, the SSTAs are accompanied by easterly wind anomalies in the equatorial Indian Ocean which favour upwelling alongshore wind anomalies off Sumatra. This pattern is however observed to reverse during the negative phase of the IODM which is much weaker than the positive phase (Saji et al., 1999; Webster et al., 1999). The IODM is reported to be phase-locked to the annual cycle in the Indian Ocean with its peak strength of the anomalies generally occurring during OND and it affects both the atmosphere and ocean (Saji et al., 1999; Webster et al., 1999). For example, droughts in Indonesia and rainfall over India, Australia and equatorial East Africa are indicated to be influenced by the IODM (Webster et al., 1999). Also, the 1961 rainfall anomaly is reported to be the consequence of the reversal in the prevailing wind regime in the Indian Ocean, positive SSTAs in the western Indian Ocean and a burst of cool air from the southern Indian Ocean (Mistry and Conway, 2003). These factors have been shown to combine and create instability in the Lake Victoria region. In 1961, the anomalous regime was similar in appearance to the event in 1997 and was maintained by the localized Indian Ocean El Niño type phenomenon (Saji et al., 1999; Webster et al., 1999).

The strongest of the known positive IODM events is reported to have occurred during 1997-98 coinciding with the most intense ENSO in recent decades. During this IODM event, the SST in the eastern Indian Ocean was shown to be cooler by more than 2°C and the western Indian Ocean was warmer by more than 2°C (Yu and Reirecker, 1999; Webster et al., 1999). It was also observed that the east-west contrast in SST in turn maintained the wind anomalies for a longer period than expected by coupled ocean-atmospheric interaction

(Webster et al., 1999; Saji et al., 1999). The wind anomalies were shown to alter the thermal structure of the equatorial Indian Ocean from its average east-west orientation. Eastward propagating Kelvin waves produced by these anomalous easterlies were shown to lift the thermocline in the eastern Indian Ocean and alongshore winds off Sumatra and subsequently enhanced the cooling in the eastern Indian Ocean (Murtugudde et al., 2000). They also found out that warming in the western Indian Ocean was caused by weak southwest monsoon winds and meridional advection and was sustained till early 1998 by a downwelling Rossby wave.

The strength of this event was manifested by the severity of the floods and destruction of properties and infrastructure caused by the accompanying rainfall (Murtugudde et al., 2000). For example in Tanzania, roads, railways, airstrips, telecommunication networks, agricultural crops and houses were damaged and destroyed over various places of the country. The impacts of these destructions were more severe in landlocked areas like central and western regions where the inflation increased tremendously to more than 100 percent. At the same time, these areas remain isolated from the rest of the country and missed important economic, social, political mitigations. The individuals and the government inevitably incurred the cost of replacing the destroyed infrastructure.

Orography and inland lakes are significant features that influence Tanzanian rainfall variability at a diurnal to seasonal scale (Asnani, 1993; Anyah and Semazzi, 2004). Among others, Lake Victoria and Tanganyika have received more attention from researchers (Podsetchine et al., 1999; Nicholson, 1999; Mistry and Conway, 2003; Anyah and Semazzi, 2004; Bergonzini et al., 2004). However, it has been indicated that the relationship between the short rains and Lake Victoria Surface Temperature (LST) is not directly proportional due to the complex interactions over the lake. These interactions include the lake-induced mesoscale circulations, topography, prevailing monsoon flow regime and the location of the ITCZ over the region that may greatly influence the rainfall patterns (Anyah and Semazzi, 2004). The importance of Lake Victoria to East Africa rainfall is emphasized by Asnani (1993) because of its size and location near the equator in the midst of mountains. Strong solar insolation causes steep temperature gradients between the lake water surface and the surrounding sloping rocky land surface. This gives rise to strong mesoscale circulation on the diurnal timescale. Lake breezes dominate during the afternoon and evening and the katabatic land breezes dominate during late night and early morning up to at least 100 kilometres from the lake shore. This circulation interacts with the synoptic flow and leads to convection up to a distance of between 150 and 200 kilometres from the lakeshore. This gives rainfall to areas such as Bukoba that are near the Lake throughout the year. The rainfall over such areas increases when the synoptic-scale circulation also favours upward motion; for example, the proximity of ITCZ creates more rainfall around Lake Victoria during April-May and November. The rainfall in these areas is least during July when the ITCZ is farthest from the Lake. During the southern hemisphere summer, the meridional arm of the ITCZ runs very roughly west of Lake Victoria and very near to it. The comparison of Lake Victoria and Tanganyika signals have been shown to synchronize and this was suggested to be accounted for by large-scale mechanisms (Bergonzini et al., 2004).

1.3 Report Organization

This report is organized into the following sections: section 2 describes the models and methodology employed in this study, data sources and analysis; section 3 presents the results; section 4 discusses the results; and section 5 presents the conclusions.

2 Model Description, Data and Methodology

The output from the HadAM3 model and the NCEP reanalysis data are compared to assess the ability of the former in adequately represent climate features in the latter. Since the core objective is to assess the ability of HadAM3 against NCEP reanalysis and GPCP data, the former is the only one described. The description of the NCEP reanalysis data, GPCP data and other data used in this study is also given in this section.

HadAM3 is a recent version of the Hadley Centre Climate model which is the result of the changes in atmospheric parametrizations made in the HadAM2b (Pope et al., 2000). The standard climate version of HadAM3 has a horizontal grid of 2.5° latitude by 3.75° longitude and 19 horizontal levels in the vertical and 30 minutes timestep. It is a hydrostatic, grid point model using an Arakawa B grid and hybrid vertical co-ordinates and use an Eulerian advection scheme. The basic features of the model are as described by Pope et al., (2000).

The major changes to the physical parametrizations included in HadAM3 are a new radiation scheme (Edwards and Slingo, 1996); convective momentum transport (Gregory et al., 1997); a new land surface scheme, Meteorological Office Surface Exchange Scheme (MOSES) (Cox et al., 1999) and the new capabilities of importance to climate research like, radiative effects of aerosols and trace gases; and the effects of carbon dioxide on evaporation at land surface.

In changing from HadAM2b to HadAM3, the model performance has shown the improvement in the mean climate and it now compares well with observation and isolates the impacts of the new physical parametrizations (Pope et al., 2000). As outlined by Pope et al., (2000), the details of the main improvements were; the improved local Mean Sea Level Pressure (MSLP) biases and changes in convective momentum transport and boundary layer; improved tropical winds; reduced tropospheric cold bias; reduced moist bias; reduced dry bias in the tropical middle troposphere; improved rainfall and circulation in the Indonesian warm pool; improved representation of the blocking in the North Pacific; improved surface and subsurface winter continental temperatures; and the most significant one in the coupled model is the is the improved surface heat fluxes.

Overall, HadAM3 has been shown to produce a good simulation of current climate when forced with observed SST (Pope et al., 2000). In addition, the inclusion of convective momentum transport and new radiation scheme has a substantial improvement of HadAM3 in the presentation of precipitation, OLR and divergent flow over tropical Indonesia. HadAM3 was also used together with observed data to study the North Atlantic Oscillation (NAO), SO and North Pacific indices and there was a fair correlation with observational indices for the SO $(r^2=0.52)$ and it was shown that the model can capture the spatial characteristics of the main modes of variability (Josey, 1999). In another investigation, HadAM3 proved to represent the impacts of the 1997/8 El Niño over southern Africa when the modulations to Angola low - a summer heat low over South Eastern (SE) Angola and North Eastern (NE) Namibia, were weak and the Indian Ocean SST forcings were strong

(Reason and Jagadheesha, 2005). A comparative study (this study) of the HadAM3 model data on one hand and the NCEP reanalysis and GPCP data on the other hand over East Africa has shown that HadAM3 is very successful during the OND season.

However, there are some outstanding errors in HadAM3. These errors include a high pressure bias over the poles; cold bias around the tropopause and related biases in the cloud distribution and optical properties; Hadley and Walker circulations are too strong; and for the coupled model the most significant errors are the excessive cooling of the ocean in the North Pacific and excessive warming in the Southern Ocean and eastern tropical oceans (Pope et al., 2000). Also, HadAM3 shows less precipitation in the tropics and increases rms error over land but decreases them over the sea. The increase of rms errors in precipitation over tropical Africa (10%) was shown and the degradations in the monsoon circulations were cited as the reason for the change. The tendency for seasonal shifts in African tropical rainfall are shown to be more marked in HadAM3, leading to increased rms errors in September to November and March to May. Monsoon westerlies are also shown to be too strong north of Malaysia in summer and too much rain over the ocean while too little over southern Africa (Pope et al., 2000). Globally, HadAM3 shows that mean changes in precipitation are small over land with rms. errors increasing slightly. In addition, when HadAM3 was used together with observed data to study the NAO, SO and North Pacific indices, it was discovered that the model poorly represents NAO index time series ($r^2=0.02$) (Josey, 1999) although it produces similar patterns. Furthermore, the model could not capture the evolution characteristics of the main modes of variability. It was also observed that HadAM3 was less successful in simulating the 1991/2 and 2002/3 El Niño over southern Africa and the model has difficulty in adequately representing the Angola low feature and its variability, therefore the model was regarded to have problems in capturing ENSO rainfall impacts over Southern Africa (Reason and Jagadheesha, 2005). Moreover, Dean et al., (2005) observed that HadAM3, with its 19 vertical levels, does not simulate sufficient high cloud over land.

Since experiments were done in attempt to reduce the remaining model errors which included improvements in vertical advection, reduction in the temperature and moisture biases in the tropopause (Pope et al., 2000). It was proposed that increasing the vertical resolution around the tropopause is one way of achieving the improvement in vertical advection. Also, recent tests with 30 vertical levels in HadAM3 have produced significant improvements in temperature and moisture in the upper troposphere. It was also suggested that the use of more accurate advection scheme could make improvements. For example, semi-Lagrangian advection has been shown to make similar or greater improvements in other models (Chen and Bates, 1996; Williamson et al., 1998). Furthermore, recent tests with improved cloud parametrization in HadAM3 have significantly reduced the cooling in the north Pacific for the errors that particularly affect the coupled model (Pope et al., 2000)

Based on the above review of HadAM3, there is an indication that the model qualifies to be used in the current study.

HadAM3 has been integrated for the 1985–2003 period with the observed Reynolds monthly SST available as global data on a 1^{o} x1^{o} latitude-longitude grid (Reynolds and Smith, 1994), as part of the University of Cape Town (UCT) seasonal forecasting project, and an ensemble of five integrations for this period has been produced in order to adequately represent the atmospheric sensitivity to different initial conditions.

Data from the area between longitudes 22.5 ^{o}E and 65 ^{o}E and latitudes 10 ^{o}N and 20 ^{o}S (precipitation and OLR) and 22.5 ^{o}E to 100 ^{o}E (geopotential heights and winds) are analysed. A larger area for geopotential heights and winds is selected get a better view of atmospheric circulations over the tropical Indian Ocean that impact rainfall over East Africa. The data needed from HadAM3 were available consistently for the period from 1985 to 2003 only. Therefore the period covered in this study is from January 1985 to December 2003. The stations from which the rainfall data were obtained are shown in Figure 1

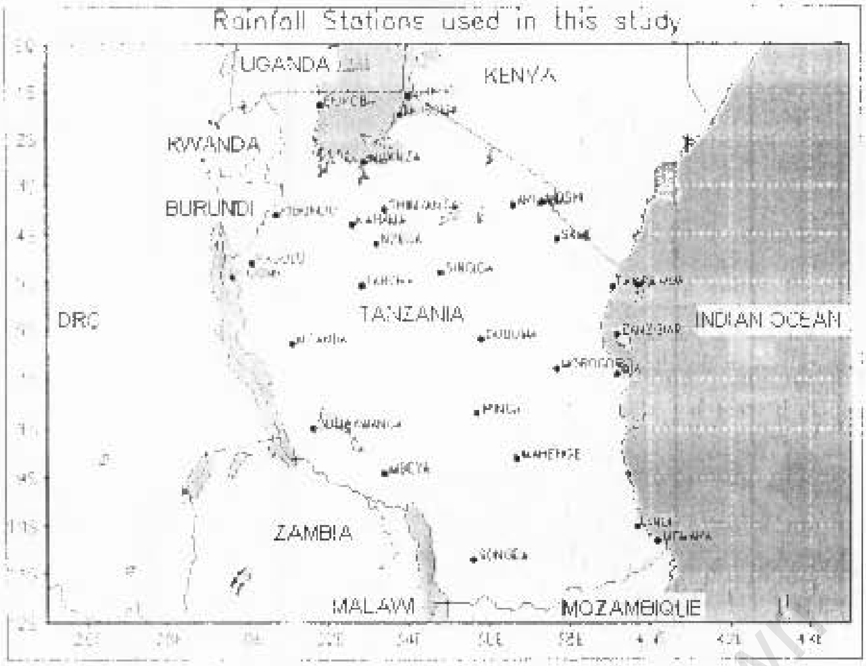

Fig. 1. The map of Tanzania showing rainfall stations used in this study

Data used for this study were obtained as daily or monthly datasets. The daily data analysed are station rainfall data from Tanzania Meteorological Agency (TMA) and HadAM3 derived OLR, precipitation, zonal and meridional winds (winds) and geopotential heights. Interpolated OLR, winds and geopotential heights from NCEP and precipitation from GPCP Version 2 Monthly Satellite-Gauge Precipitation Data Set comprise the monthly data used. Monthly precipitation from Climate Research Unit (CRU) 2.1 dataset is used to derive the interannual timeseries and consider the potential decadal variability present in the OND and MAM seasons.

The NCEP Reanalysis data used are provided by the NOAA/OAR/ESRL PSD, Boulder, Colorado, USA, from their Web site at http://www.cdc.noaa.gov/. NCEP and National Centre for Atmospheric Research (NCAR) cooperated in a project to produce a 40-year record of global analyses of atmospheric fields in support of the needs of the research and climate monitoring communities (Kalnay et al., 1996). This effort involves the recovery of land surface, ship, rawinsonde, pibal, aircraft, and satellite, quality controlling and assimilating these data with a data assimilation system which is kept unchanged over the reanalysis period 1957 through 1996. This eliminates perceived climate jumps associated with changes in the data assimilation system. The NCEP/NCAR 40-year reanalysis uses a frozen state-of-the-art global data assimilation system, and a data base as complete as possible. The data assimilation and the model used are identical to the global system implemented operationally at NCEP on 11 January 1995, except that the horizontal resolution is T62 (about 210 km). The data base has been enhanced with many sources of observations not available in real time for operations, provided by different countries and organizations. However it has been noted that there are few observations over Africa so as a result, the NCEP Reanalysis data may not be that accurate over East Africa.

GPCP is an element of the Global Energy and Water Cycle Experiment (GEWEX) of the World Climate Research program (WCRP). It was established by the WCRP in 1986 with the initial goal of providing monthly mean precipitation data on a 2.5°× 2.5°latitude-longitude grid (Adler et al., 2003). Monthly mean precipitation estimates are available from 1979 to 2005. The GPCP has accomplished this by merging infrared and microwave satellite estimates of precipitation with rain gauge data from more than 6,000 stations. Infrared precipitation estimates are obtained from Geostationary Satellite Server (GOES) (United States), Geostationary Meteorological Satellite (GMS) (Japan) and Mid-Earth orbit Earth Observing Satellite (MEOSAT) (European Community) geostationary satellites and National Oceanic and Atmospheric Administration (NOAA) operational polar orbiting satellites. Microwave estimates are obtained from the U.S. Defense Meteorological Satellite Program (DMSP) satellites using the Special Sensor Microwave Imager (SSM/I).

The CRU TS 2.1 dataset comprises 1224 monthly grids of observed climate, for the period 1901-2002, and covering the global land surface at 0.5 degree resolution (Mitchell and Philip, 2005). There are nine climate variables available in this dataset which are daily mean, minimum and maximum temperature; diurnal temperature range; precipitation; wet day frequency; frost day frequency; vapour pressure and cloud cover.

The above data were analysed to obtained monthly and seasonal means and anomalies for respective years, monthly and seasonal climatologies (climatological means) and interannual variability. Empirical Orthogonal Functions (EOF) and Principal Component Analysis (PCA) are used to give an indication of the spatiotemporal distribution of rainfall, geopotential heights and OLR.

Monthly means were calculated by averaging daily data into respective months. The obtained monthly data were averaged into respective seasons to provide for seasonal means in respective years. Monthly and seasonal climatological means were obtained by averaging the respective monthly and seasonal means. The anomalies were then calculated by subtracting respective monthly and seasonal means from their respective monthly and seasonal climatological means. The interannual variability, EOF and PCA for each season were then obtained from their respective anomalies.

The derived variables are calculated as shown below;

A mean (μ_x) of variable (X) is give by $\mu_x = \frac{\sum_{i=1}^{n} X_i}{n}$, where n is the total number entries of variable (X)

An anomaly (A) is given by $A = \mu_x - X_i$.

The PCA and EOF are obtained from the computation of the eigenvalue matrix (D) and the eigenvector matrix (V) of the covariance matrix C, by solving this equation: $C \bullet V = D \bullet V$.

Two seasons were picked for analysis, which are October to December (OND) and March to May (MAM) (Fig. 2). Seasonal anomalies were used to assess interannual variability potentially present in the record (Fig. 4). Dry, average and wet years were delineated by considering the rainfall anomalies less than -10mm per month as dry, greater than 10mm per month as wet and those between the two as average (Fig. 4). These criteria were used in consideration to the economic importance of rainfall to Tanzania.

3 Results

Results showing the monthly and seasonal rainfall climatology, interannual and decadal rainfall variability, seasonal vector winds climatology and EOF and PCA of precipitation, geopotential height and OLR over East Africa and western tropical Indian Ocean are presented in this section.

3.1 Monthly Rainfall Climatology

Over unimodal areas, the rains start in October and end in late April to early May while over bimodal areas, short rains start in October and cease in December and the long rains begin March and end in May (Mhita, 2003; Fig. 2). These onset and cessation periods follow the arrival and departure of the ITCZ over those areas (Asnani, 1993). The areas in the vicinity of Indian Ocean, Great Lakes, North and Southern Highlands, and Eastern Arc Mountains are indicated as receiving more rainfall in terms of intensity and duration than the rest of the country due to the local influence of these features (Fig.2). The local influence of orography and large water bodies on the intensity and duration of rainfall over the nearby areas is also explained by Asnani (1993)

The 1985-2003 station rainfall monthly climatology indicates that the rain season over most of the country starts mainly during October for unimodal areas, late October and March for bimodal areas and ends mainly in late April or early May for unimodal areas and December and May for bimodal areas (Fig.2). Over the unimodal areas, the rainfall peaks for the first time mostly in December or January and again in March. On the other hand, rainfall peaks during November over the bimodal areas during the short rains season and in March during the long rain season. Over most of the bimodal areas, more rainfall occurs during the MAM season than the OND season. On the other hand, much more rainfall is experienced during December, January, February and March than for the other months over the unimodal areas. It is therefore evident that rainfall seasonality follows the position of the ITCZ meridional arm over the country (Asnani 1993).

In comparing the GPCP and HadAM3 model seasonal precipitation climatology (Fig. 3), it was evident that the model is capable of depicting the essential precipitation patterns. However, the model seems to underestimate precipitation in both MAM and OND over land and overestimate it over the ocean (Fig. 3). It was also noted that the model shows too little precipitation over the northern highlands and incorrectly indicates that this area is relatively dry compared to the rest of the country. The influence of the ocean and great lakes on the amount of precipitation received over the adjacent areas is stronger in the MAM season and GPCP than in the OND season and HadAM3 model. Orographic influences are not clearly detected and this may have been obscured by the coarse spatial resolutions of the model and GPCP data which are not able to capture mesoscale rainfall variability.

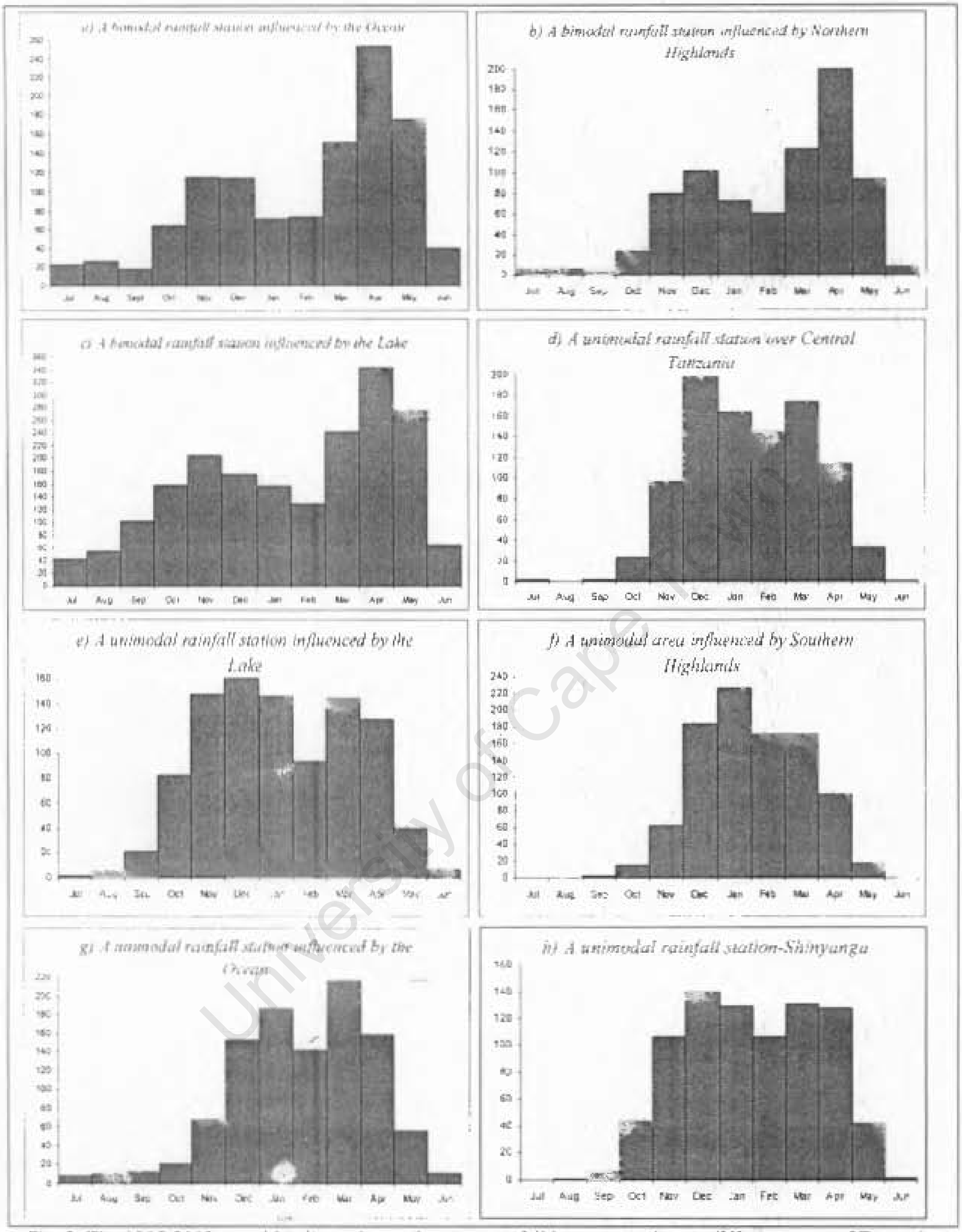

Fig. 2. The 1985-2003 monthly climatology of station rainfall in <u>mm/month</u> over different areas of Tanzania, the station names are: a) Dar es Salaam, b) Arusha, c) Bukoba, d) Dodoma, e) Kigoma, f) Mbeya and g) Mtwara. (Note that the vertical scales in each panel are different)

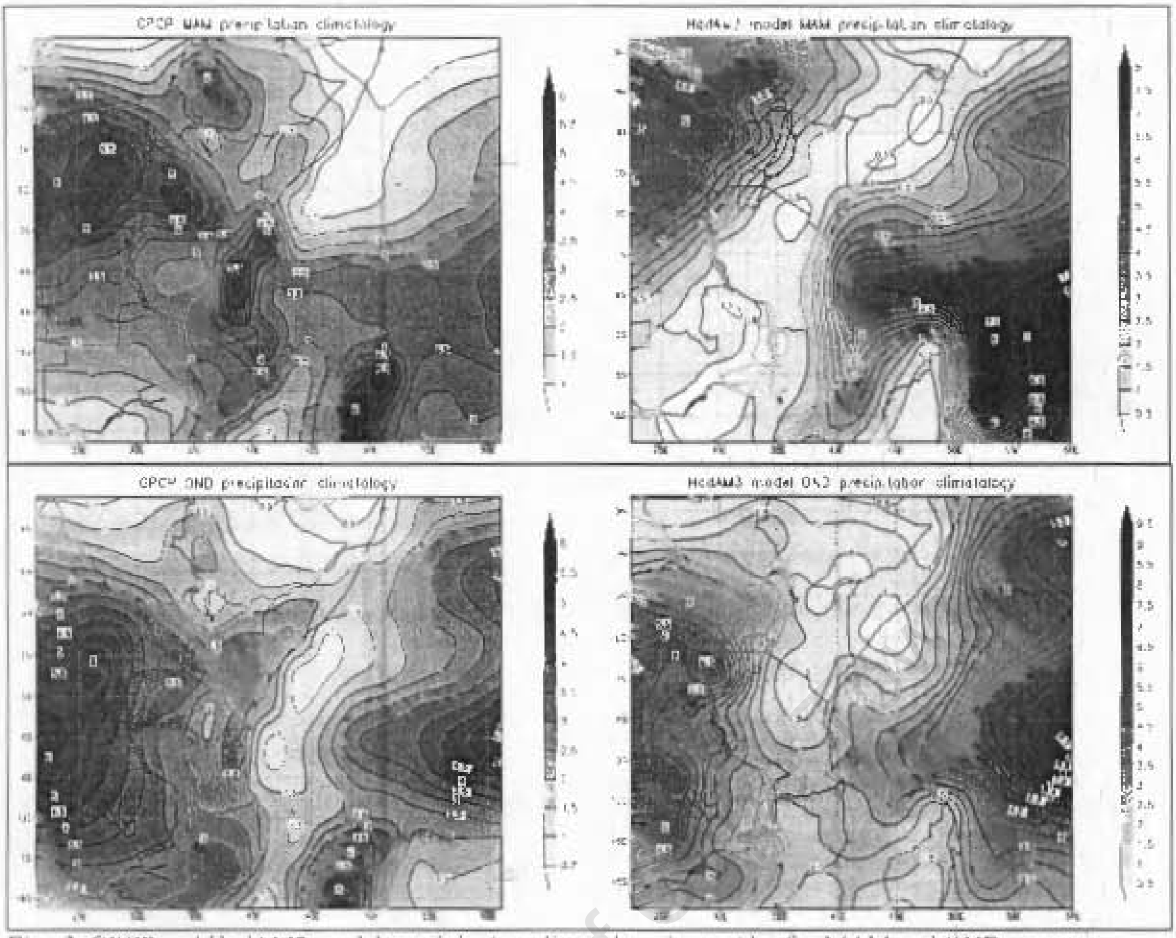

Fig. 3. GPCP and HadAM3 model precipitation climatology in *mm/day* for MAM and OND seasons

3.2 Interannual Rainfall Variability

The analysis of TMA station rainfall data (see fig. 1 for rainfall stations used) for 1985-2003 showed some exceptionally wet and dry seasons over Tanzania during this period (Fig. 4). Examining the wet and dry years, it is noted that the wettest year for MAM season is 1986 while the driest one is 2003 while for OND the wettest year is shown to be 1997 and 1993 is the driest (Fig. 4). Additionally, there seems to be a tendency for some of the episodes to occur in both seasons consecutively, for example, it was wet in MAM 1986 as well as in OND 1986 and the same can be seen for 1993 and 2003 in which the seasons were both dry. Some of these remarkably dry/wet years are noted to be ENSO events, for example, the OND of 1986 and 1997 were El Nino episodes (Fig. 4). During the OND 1997 season, anomalously high amounts of rainfall were recorded over East Africa. Over Tanzania, the most anomalous amount of rainfall was observed over the northeastern coast and the least anomalous occurred over the southwestern areas (Fig. 5). The consecutive occurrence of dry episodes in 2001 and 2003 have to some extent aggravated the severity of water shortage in the country (Fig. 4).

The rainfall timeseries derived from CRU 2.1 TS dataset for Tanzania (12S to 0 and 30E to 41E) (Fig. 7) suggests the less than average rainfall mainly occurred during 1981-2000 for MAM. On the other hand, for OND, above to near average rainfall mainly occurred during 1961-2000 with less rainfall in the last decade (1991-2000) than in the previous one (1981-1990). In addition, a ten year moving average depicts a slight decrease in the amount of rainfall received over the country after 1997/98 in both seasons (Fig. 6). The analysis indicates that there seems to be less rainfall received over Tanzania in the last decade (ending 2005) than in the previous one. This is in agreement with the recent shortage of rainfall experienced over the many parts of country and it adversely impacted the agriculture, water management and power supply sectors accordingly. However, above average rainfall has been reported all over the country during the OND season of 2006 and this may be attributed to the weak ENSO event reported to be prevailing at that time.

A likely influence on the interannual variability during OND as opposed to MAM may be in connection to strong interannual signals found in SSTAs which seems to affect rainfall more strongly during the former season than the latter one (Fig. 4; Fig. 6). It is also noted that more rainfall is experienced during the MAM season than during the OND season. More rainfall received during the MAM season may be attributed to the length of the season and high intensity of rainfall during this season.

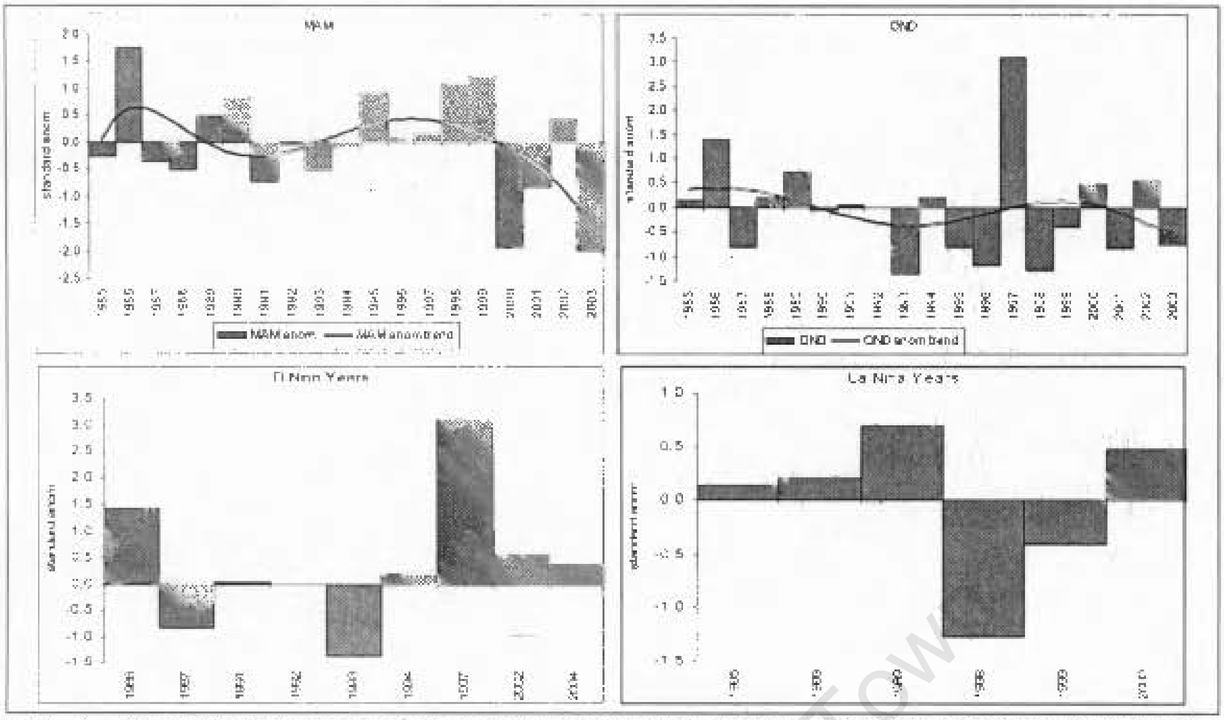

Fig. 4. Standardized departures of interannual station rainfall variability over Tanzania, the figure shows on the top left variability during the MAM season, top right variability during the OND season, bottom left El Nino years and bottom right La Nina years. (Note that the vertical scales in each panel are different)

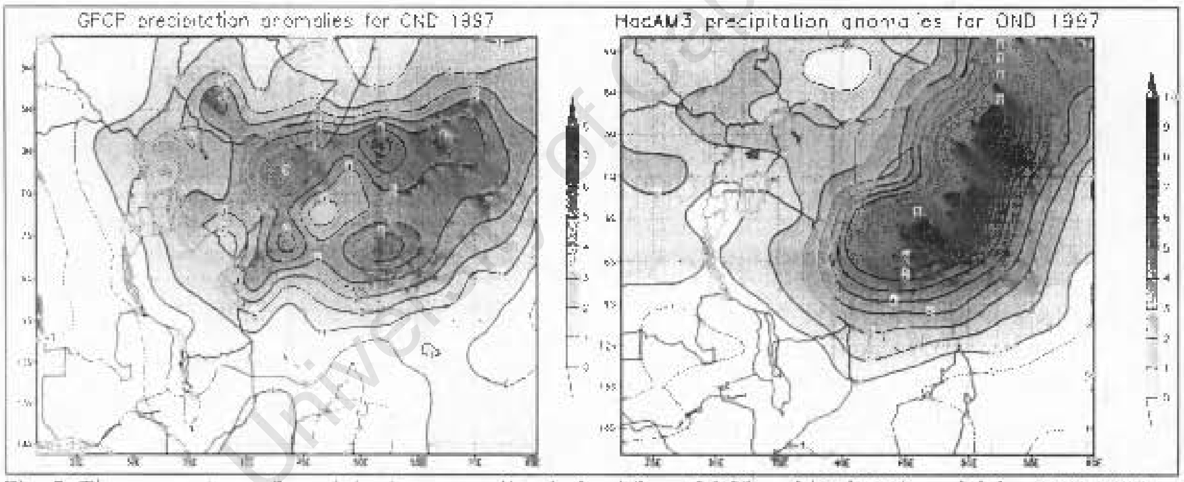

Fig. 5. The comparison of precipitation anomalies derived from GPCP and HadAM3 model for OND 1997

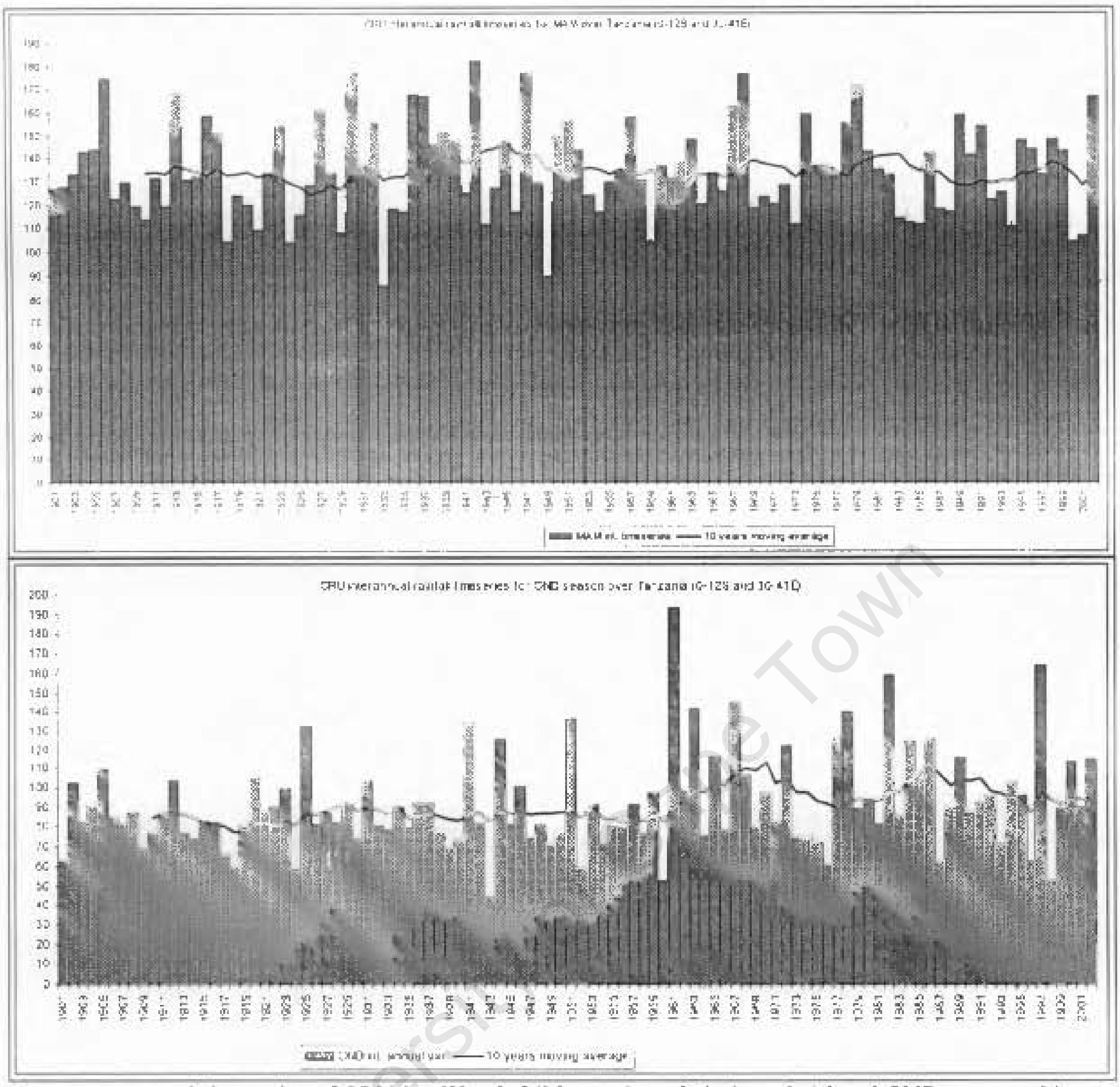

Fig. 6. Interannual timeseries of CRU 2.1 TS rainfall in *mm/month* during MAM and OND season with a ten year moving average. (Note that the vertical scales in each panel are different)

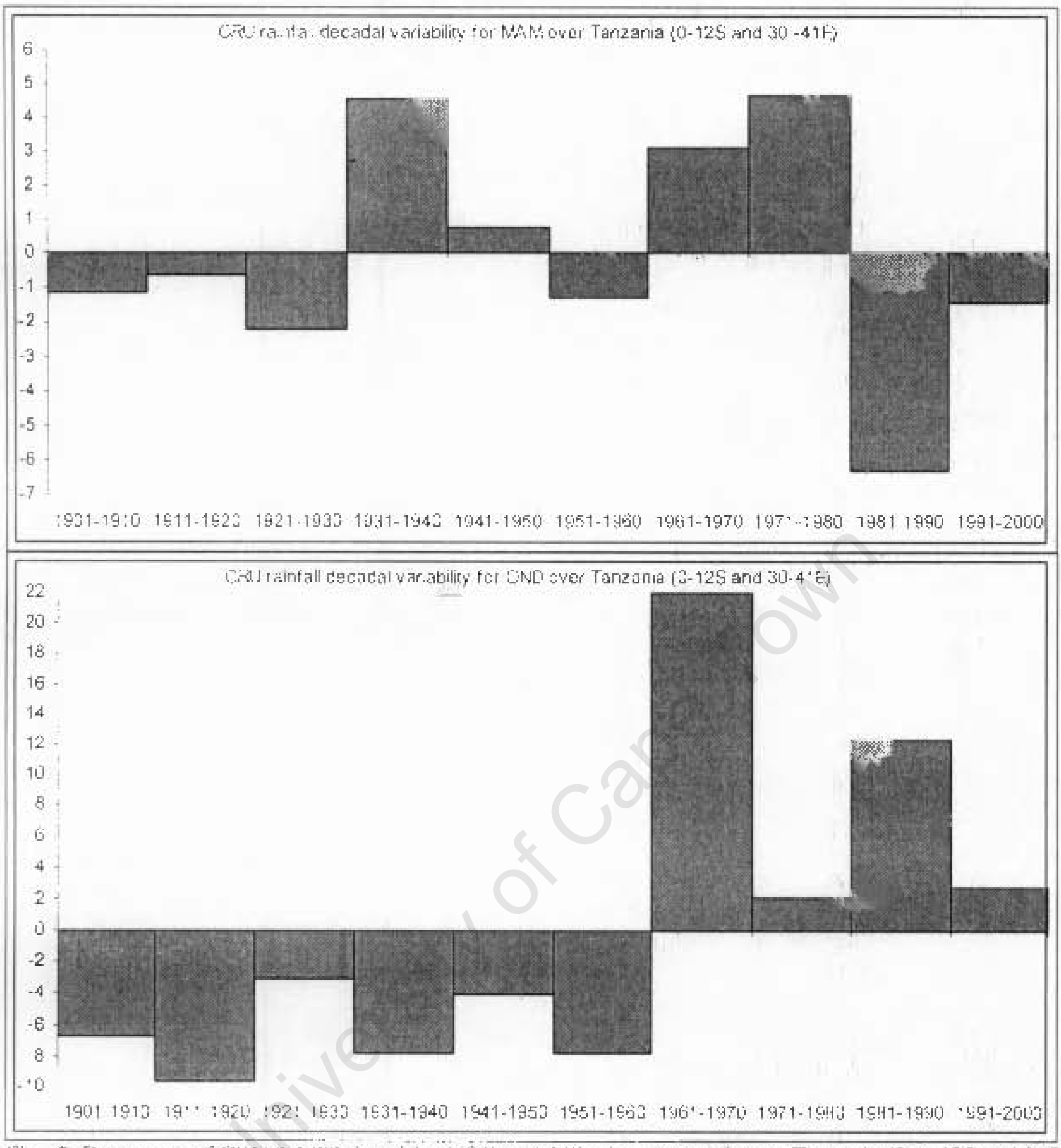

Fig. 7. Departures of CRU 2.1 TS decadal rainfall variability in mm/month over Tanzania (0 to 12S and 30E to 41E) during MAM and OND seasons. (Note that the vertical scales in each panel are different).

3.3 Comparison of HadAM3 and NCEP Vector Winds Climatology during OND and MAM

Comparing the 850hPa and 200hPa vector winds climatology derived from HadAM3 and NCEP during OND and MAM, suggests that the two models reveal some differences (Fig. 8-11). For example, in MAM, the Somali Jet which is expected to start being noticeable in May and June (Anyamba and Kiangi, 1985) seems to come earlier and much stronger in HadAM3 than in NCEP (Fig. 8). As this jet tends to deviate the Indian Ocean moist air away from East Africa, it may weaken the rains during MAM in HadAM3. Off the coast of Somalia, HadAM3 shows weaker easterlies at 850hPa in MAM and the same is seen off the coast of East Africa in OND. These weaker easterlies in HadAM3 may suggest that this model may be less successful in representing East African rainfall. It is however obvious that the difference between the two models is stronger in MAM than in OND (Fig. 8-11). Therefore, it is most likely that fewer agreements between the models may be observed in MAM than in OND.

However, both models show that the winds are either reversed or weaken at 200hPa as compared to 850hPa (Fig. 8-11). For example, at 850hPa, relative convergence is shown in both models in the Indian Ocean off the coast of East Africa and relative divergence is shown over East Africa. On the other hand, the opposite is shown at 200hPa. It is therefore expected that more rain will fall over the Indian Ocean than over East Africa. This condition may be more evident in HadAM3 than in NCEP because the former has weaker easterlies than latter.

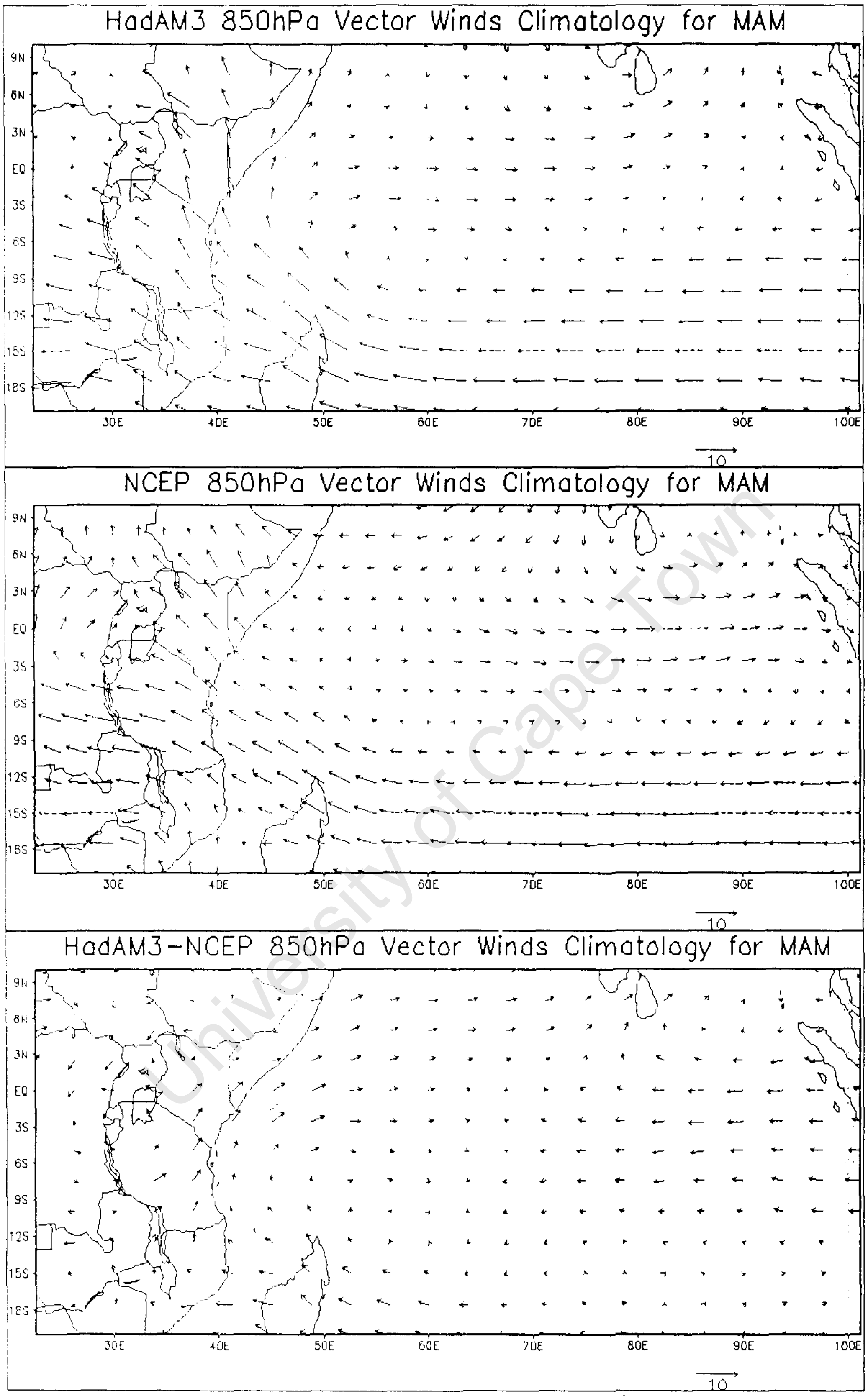

Fig. 8. HadAM3 and NCEP 850hPa vector winds climatology and their difference for MAM (A scale vector of 10 m/s is shown at the bottom of each panel)

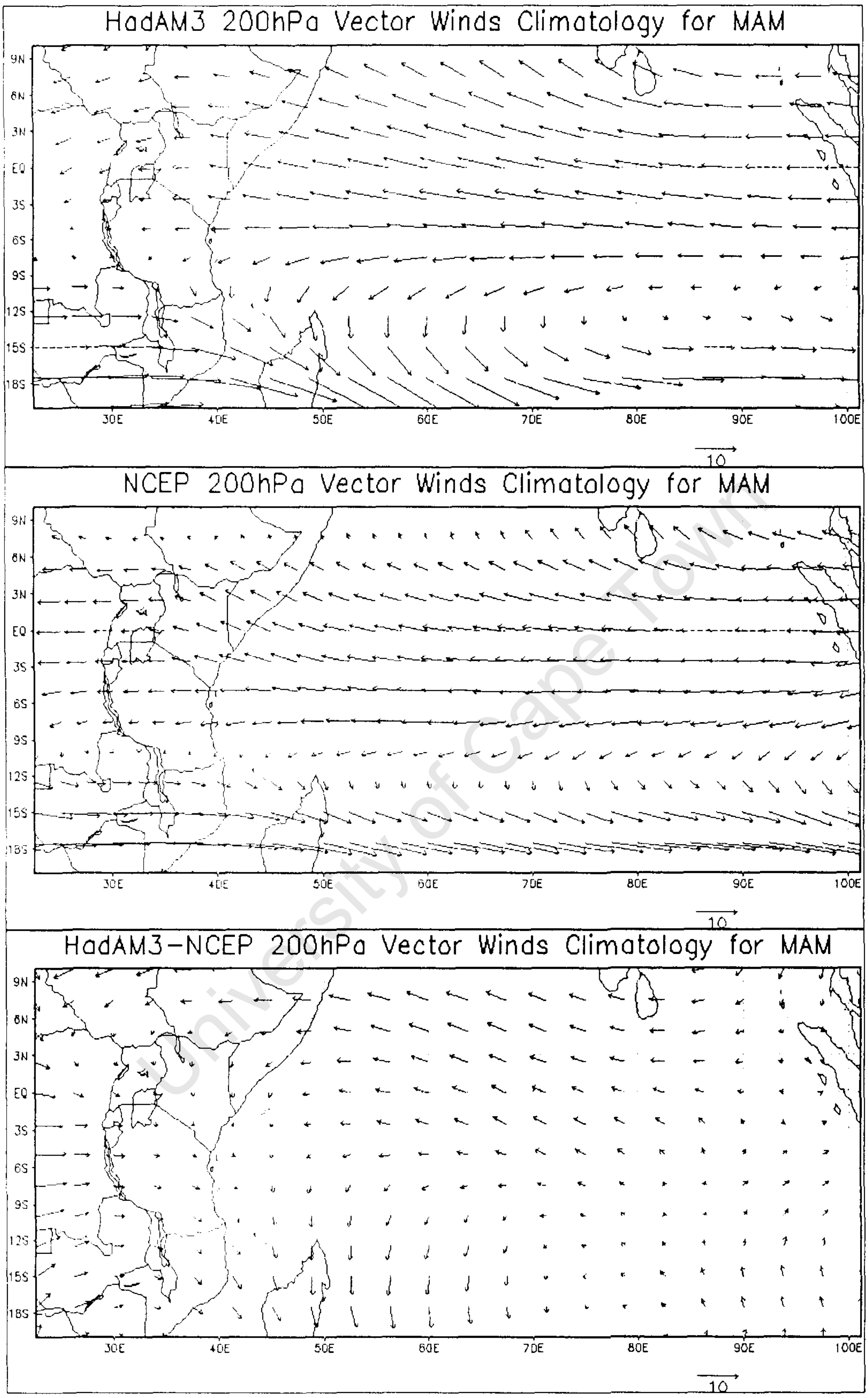

Fig. 9. HadAM3 and NCEP 200hPa vector winds climatology and their difference for MAM (A scale vector of 10 m/s is shown at the bottom of each panel)

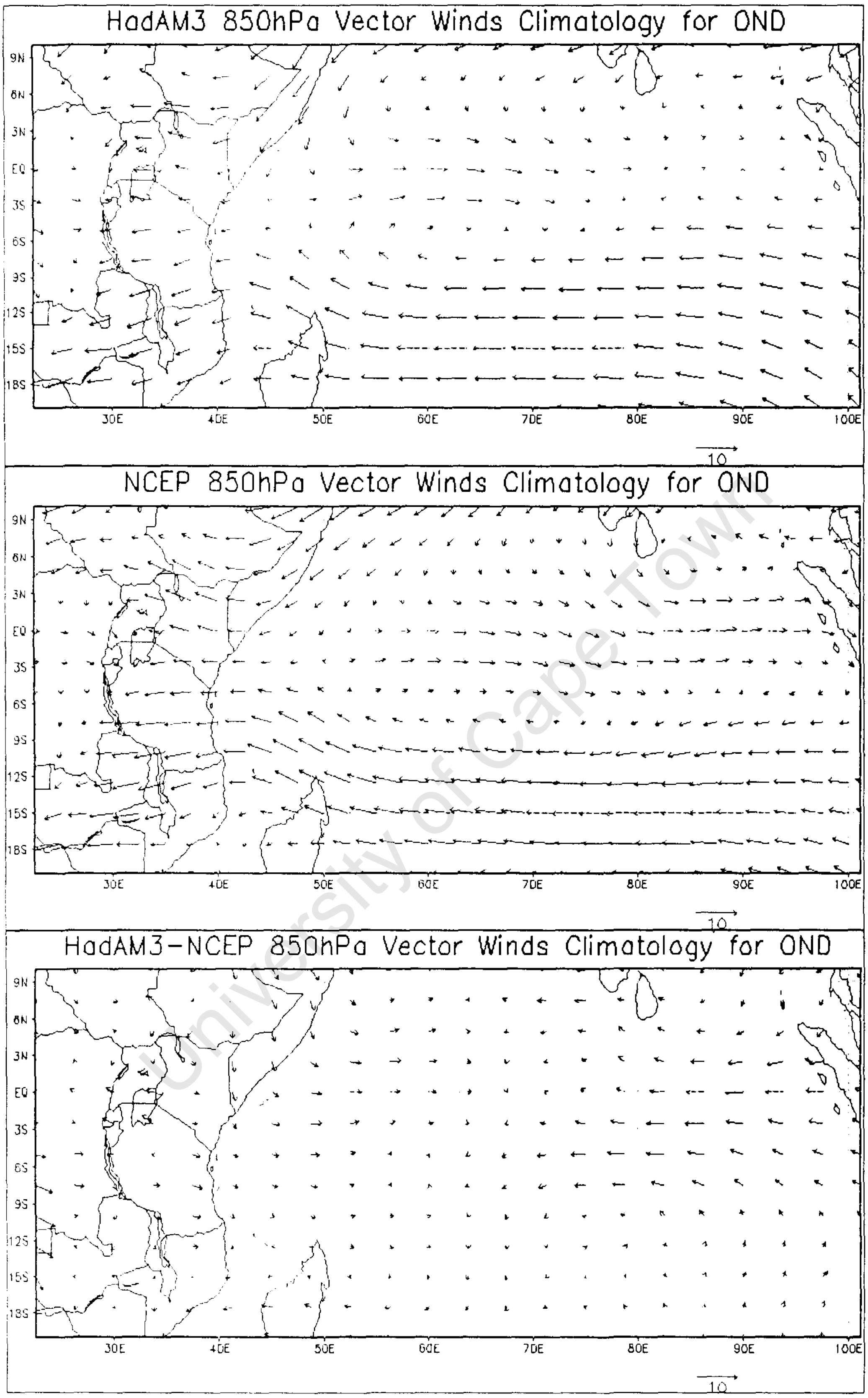

Fig. 10. HadAM3 and NCEP 850hPa vector winds climatology and their difference for OND (A scale vc ' .r of 10 m/s is shown at the bottom of each panel)

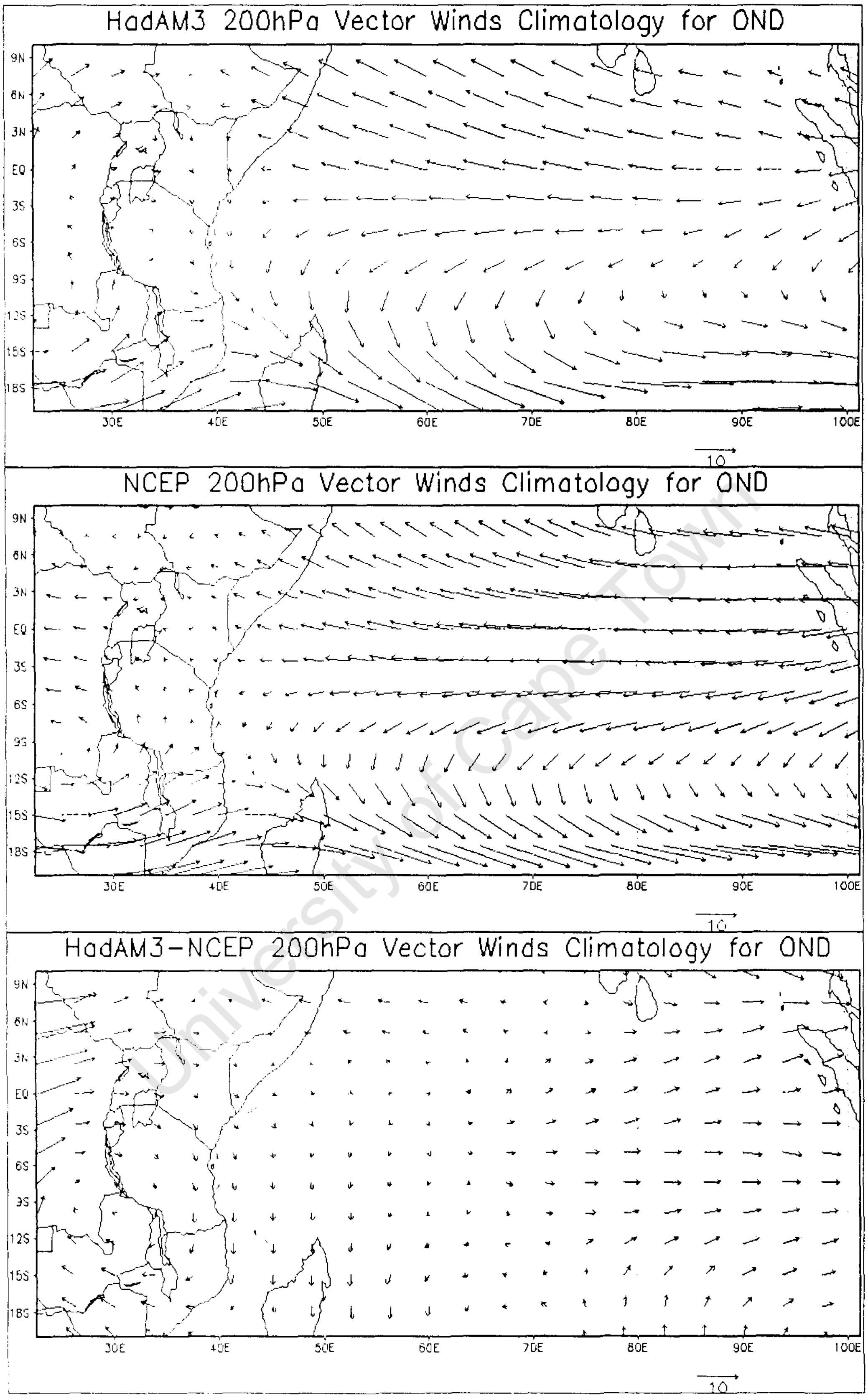

Fig. 11. HadAM3 and NCEP 200hPa vector winds climatology and their difference for OND (A scale vector of 10 m/s is shown at the bottom of each panel)

3.4 Empirical Orthogonal Functions (EOFs) and Principal Component Analysis (PCA)

Most spatiotemporal patterns of variability during OND and MAM seasons are contributed by the first PCA/EOF of NCEP reanalysis data /GPCP data and HadAM3 model data. It is therefore useful to present and discuss only the leading PCA/EOF (the second and third PCA/EOF are provided in the appendix)

The EOF and PCA derived from the 1985-2003 HadAM3 model OND and MAM 850 and 200 hPa geopotential height, OLR and precipitation anomalies were compared with those from NCEP i.e. geopotential height and OLR and GPCP i.e. precipitation to assess their spatial and temporal patterns of variability. It is noted that spatiotemporal patterns of variability shown by the HadAM3 model as compared to those of GPCP or NCEP during OND and MAM (Fig. 12-27) are evidently biased to any of the two seasons. However, some patterns seem to be variable dependent. Therefore the examination of each variable in each season may give a good reflection of the HadAM3 model ability to present East African rainfall variability in each respective season as compared to GPCP data and NCEP reanalysis data. Figure 12 to 19 are for the spatiotemporal variabilities depicted during OND while figure 20 to 27 are for those during MAM.

Comparing the leading EOF derived from GPCP and HadAM3 model precipitation anomalies during the OND season show spatially extended positive patterns in both sources over East Africa and western equatorial Indian Ocean (Fig.12). The given patterns seem to suggest that HadAM3 overestimates rainfall over the ocean but underestimates it over the land.

Close matches are noted in the first PCA of the OND season precipitation anomalies of GPCP and HadAM3 model for years between 1993 and 1998; and 2001 and 2003 (Fig. 13). The model therefore seems to show some ability in presenting temporal patterns of rainfall variability shown by GPCP data in OND.

The NCEP reanalysis and HadAM3 model OLR EOF patterns reveal noticeably different patterns of variability over East Africa and western equatorial Indian Ocean (Fig. 14). Comparing the first EOF from these two sources, the NCEP OLR EOF shows negative patterns dominating the land and the ocean while the HadAM3 model shows negative patterns over southern Zambia, Mozambique and Madagascar; and positive patterns over East Africa and western tropical Indian Ocean. Several coherent patterns of variability can be identified over the land and ocean in the NCEP OLR EOF patterns while in the HadAM3 model only two notably large patterns are shown in the Indian Ocean. The given patterns may suggest that HadAM3 seems to be biased in presenting convective systems, that is, it overestimates them over the ocean and underestimates them over land.

There is less agreement in the patterns of temporal variability between the NCEP and HadAM3 model OND OLR PCA. The only loosely matched patterns are shown between the year 1991 and 1993 (Fig. 15). It can therefore be suggested that HadAM3 model and NCEP reanalysis display little agreement in presenting OLR temporal variability during OND.

NCEP and HadAM3 show relatively similar patterns of 850hPa geopotential height anomalies first EOF variability but of different magnitude, negative geopotential height anomalies EOF patterns are shown to be dominant in NCEP model contrasting those shown in HadAM3 model (Fig. 16). Some loosely matched temporal patterns of variability can be seen between 1986 and 1988; 1996 and 1999; and 2000 and 2002 (Fig. 17). This may serve as an indication that HadAM3 and NCEP share some similarities in presenting temporal variability of geopotential heights.

Negative EOF patterns of 200hPa geopotential height anomalies dominate the leading NCEP EOF while the positive ones are dominant in the HadAM3 model (Fig. 18). Similar weaker patterns of spatial variability are depicted by NCEP and HadAM3 over East Africa. It is again evident that HadAM3 and NCEP display relatively similar spatial patterns of geopotential height variability with contrasting magnitude.

A relatively consistent match is shown by the spatial patterns of the leading PCA of 200hPa geopotential height when comparing NCEP and HadAM3 (Fig. 19). Even though the temporal patterns are not perfectly matched the general trend of variability agrees closely indicating some agreement between HadAM3 and NCEP in this case.

The patterns of spatial and temporal variability revealed during MAM by the leading EOF and PCA of the anomalies derived from GPCP and NCEP on one hand and HadAM3 on the other hand have shown the following patterns (Fig. 20-27).

The leading EOF of precipitation anomalies derived from GPCP and HadAM3 model show patterns that are contrasted (Fig. 20). While the GPCP precipitation anomalies EOF indicate the presence of a large system of positive EOF patterns over the East Africa, the HadAM3 model shows negative patterns. This may suggest that there is less agreement between GPCP and HadAM3 model in presenting spatial variability patterns of precipitation anomalies in MAM than in OND.

Temporal comparison of the GPCP and HadAM3 model precipitation anomalies leading PCA revealed a very loose match (Fig. 21). A loose match may be seen between 1993 and 2000 (Fig.21), and this seems to overlap with the close match shown during the OND season (Fig. 13). This may be substantiating the previous suggestion that there is less agreement between GPCP and HadAM3 model in presenting variability patterns of precipitation anomalies in MAM than in OND.

Contrasting OLR EOF patterns are identified over northern Tanzania and the rest of East Africa in the leading EOF of the NCEP and HadAM3 models (Fig. 22). The negative EOF patterns are dominant over the whole of East Africa in HadAM3 and southern Tanzania, Mozambique, Zambia and the Democratic Republic of Congo (DRC) in NCEP. Comparing the temporal variability of the NCEP and HadAM3 OLR leading PCA reveal a less coherent pattern in which the only matches are shown between 1985 and 1987, and between 1999 and 2003 (Fig. 23). This augments a suggestion that there is a less agreement between the OLR patterns of variability depicted by the HadAM3 model to those of the NCEP model over East Africa.

Relatively similar spatiotemporal patterns of variability are shown when comparing the HadAM3 and NCEP 850hPa and 200hPa geopotential height leading EOF and PCA (Figs. 24-27). This may be indicating that there is a comparatively better agreement between HadAM3 and NCEP models in capturing the spatiotemporal patterns of 850hPa and 200hPa geopotential height variability in MAM than in OND over East Africa.

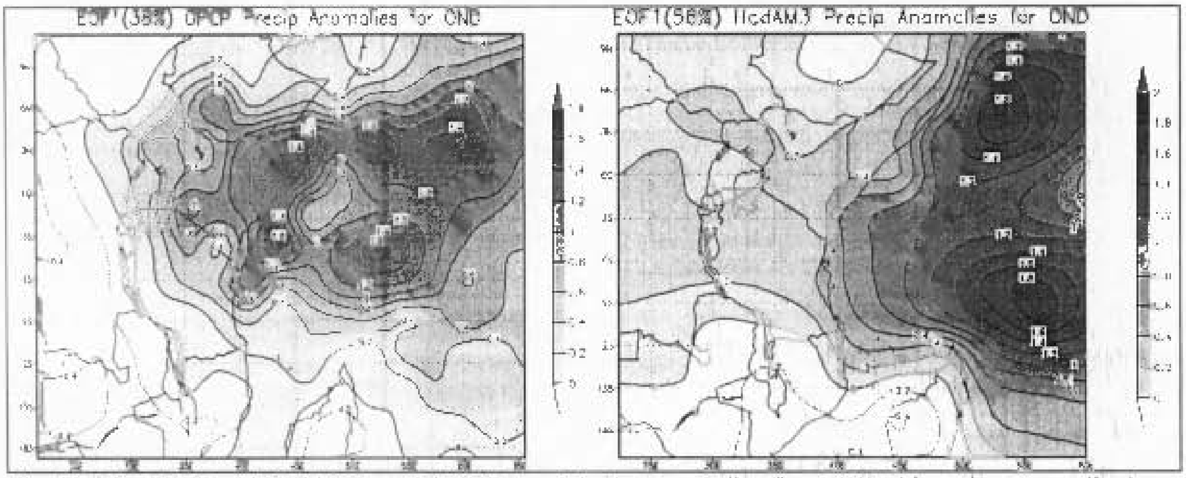

Fig. 12. The GPCP and HadAM3 model OND precipitation anomalies first EOF with variance contribution of 38% and 56% respectively, the positive EOFs are shaded.

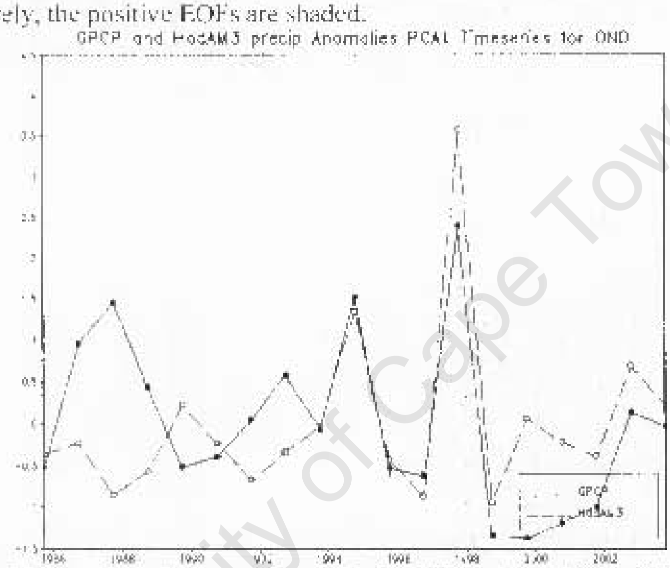

Fig. 13. Interannual variability of precipitation anomalies first PCA derived from GPCP and HadAM3 model for OND season

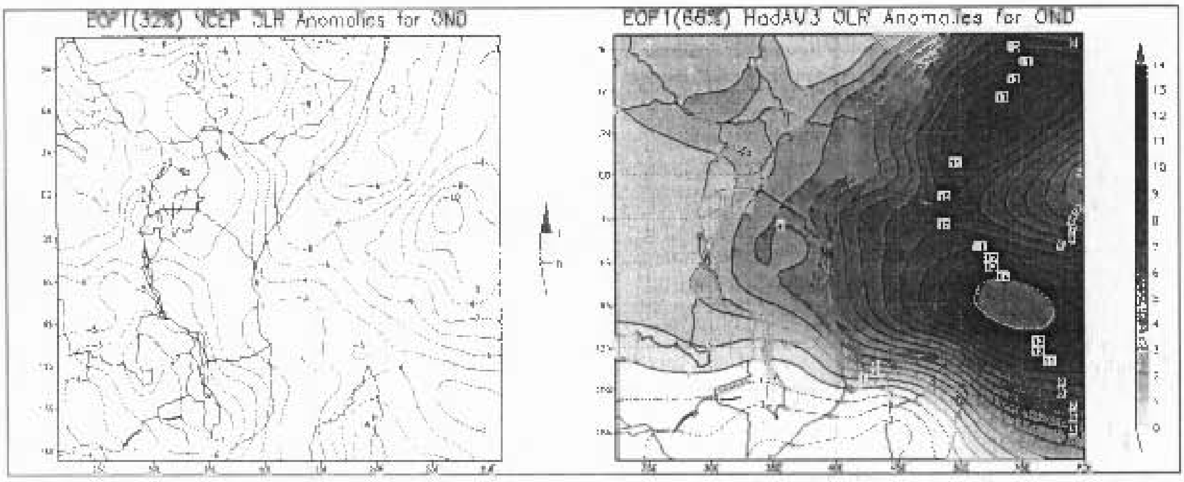

Fig. 14. The NCEP and HadAM3 model OND OLR first EOF with variance contribution of 32% and 66% respectively, the positive EOFs are shaded.

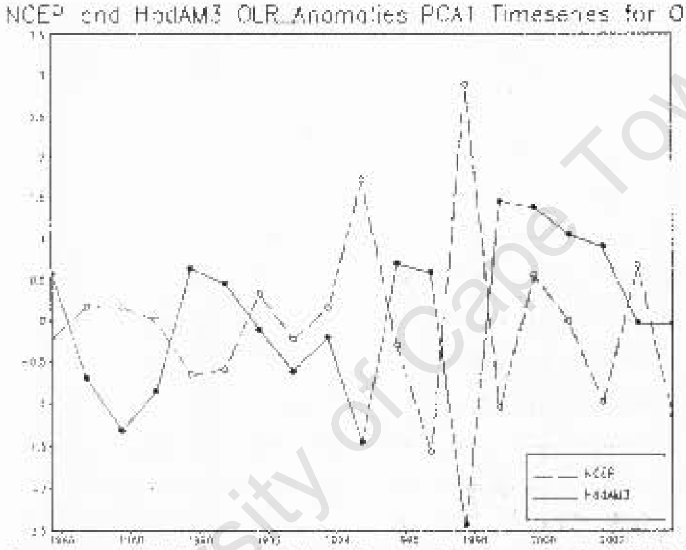

Fig. 15. Temporal patterns of NCEP and HadAM3 model OLR anomalies PCA for the OND season.

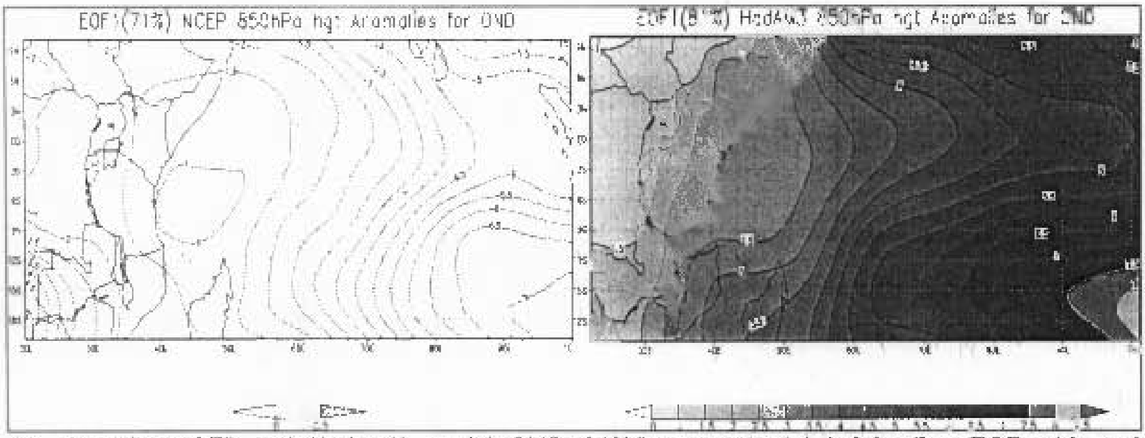

Fig. 16. The NCEP and HadAM3 model OND 850hPa geopotential height first EOF with variance contribution of 71% and 81% respectively the positive EOFs are shaded

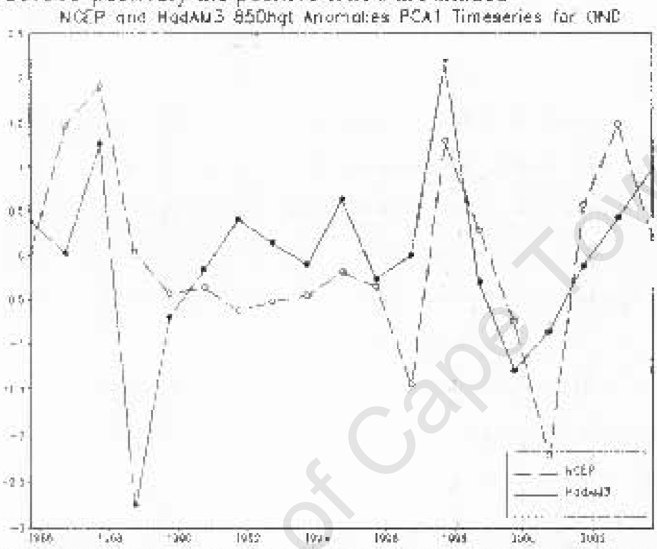

Fig. 17. Temporal patterns of NCEP and HadAM3 model 850hPa geopotential height anomalies PCA for the OND season

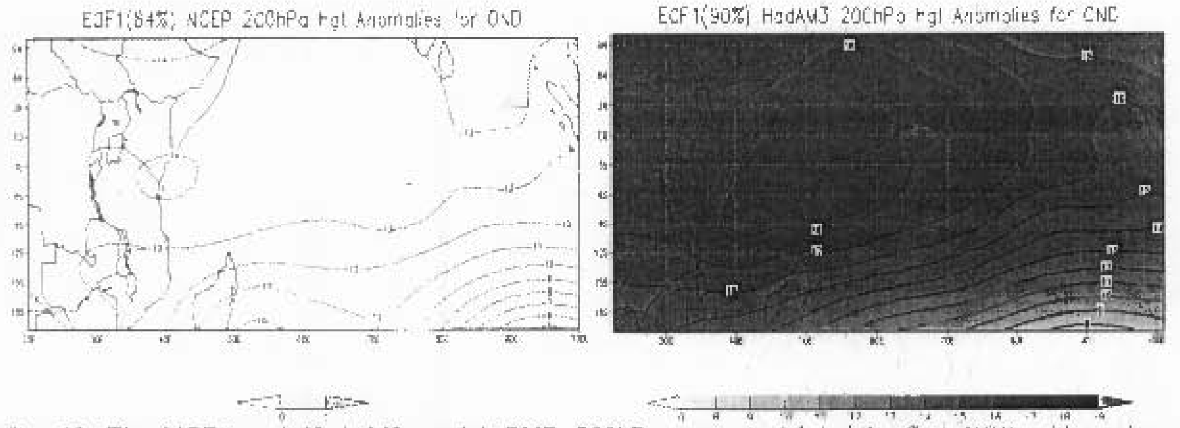

Fig. 18. The NCEP and HadAM3 model OND 200hPa geopotential height first EOF with variance contribution of 84% and 90% respectively, positive EOFs are shaded.

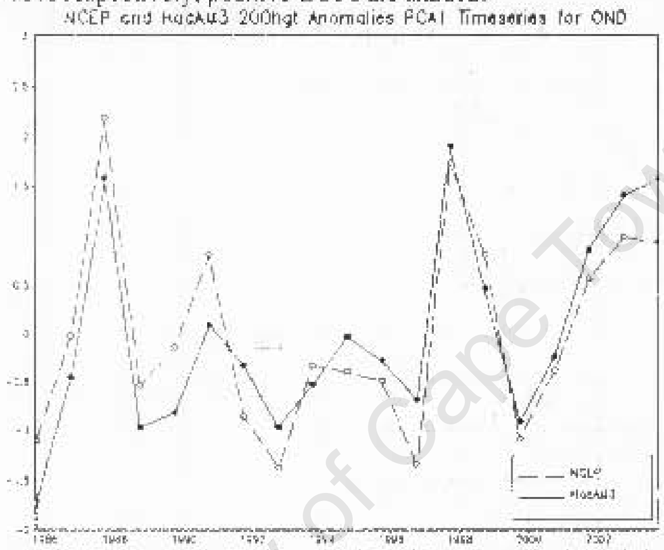

Fig. 19. Temporal patterns of NCEP and HadAM3 model 200hPa geopotential height anomalies first PCA for the OND season.

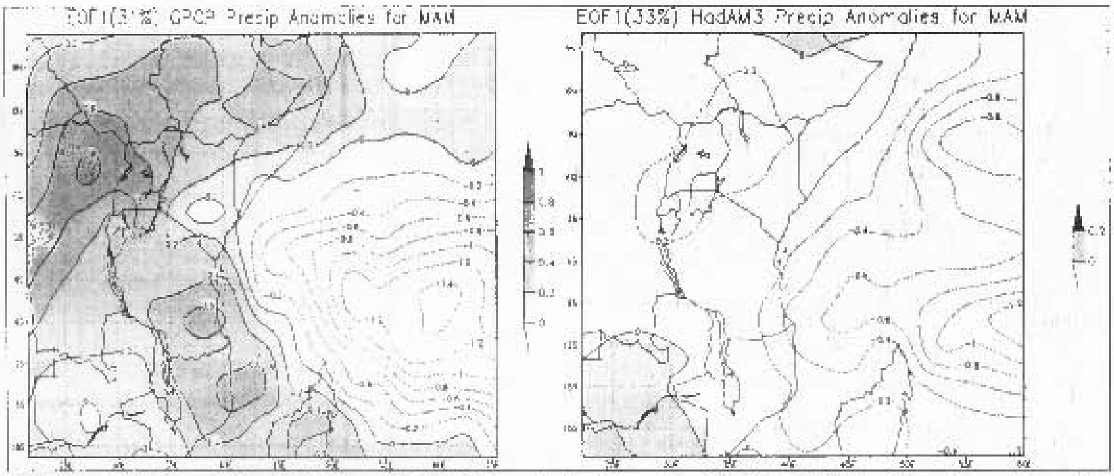

Fig. 20. The GPCP and HadAM3 model MAM precipitation anomalies first EOF with variance contribution of 31% and 33% respectively, positive EOFs are shaded.

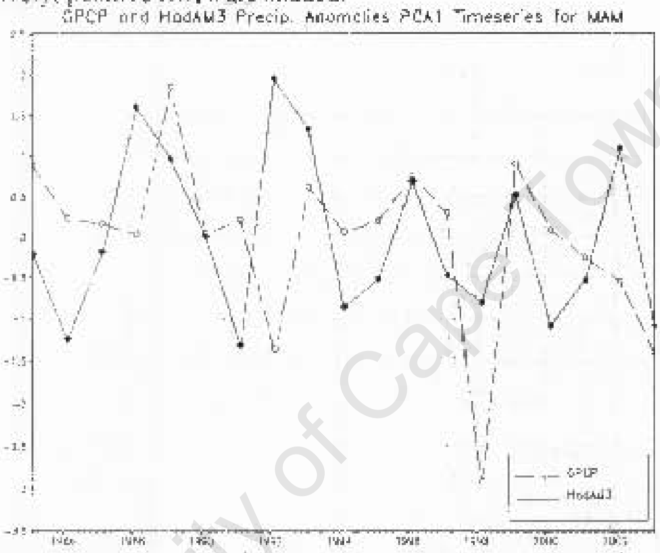

Fig. 21. Temporal patterns of GPCP and HadAM3 model precipitation anomalies first PCA for the MAM season.

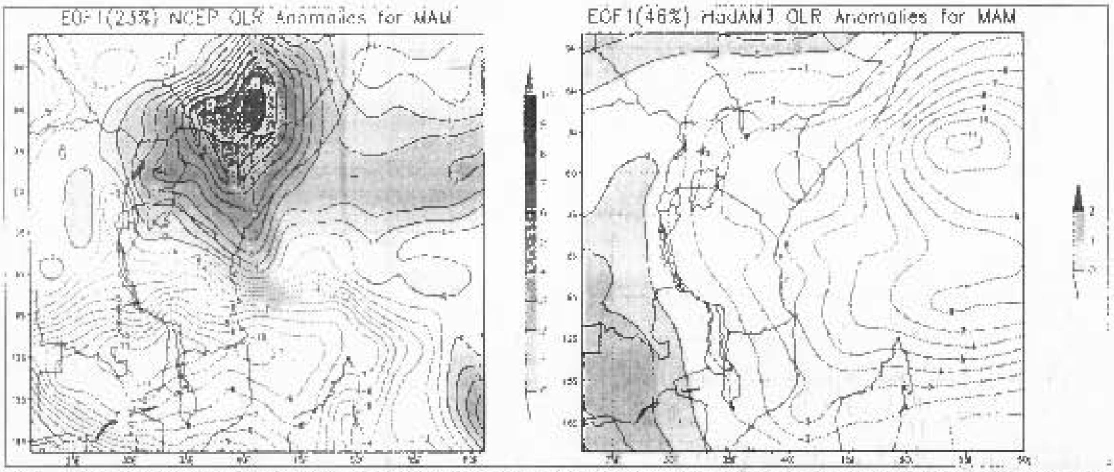

Fig. 22. The NCEP and HadAM3 model MAM OLR anomalies first EOF with variance contribution of 23% and 46% respectively, positive EOF are shaded.

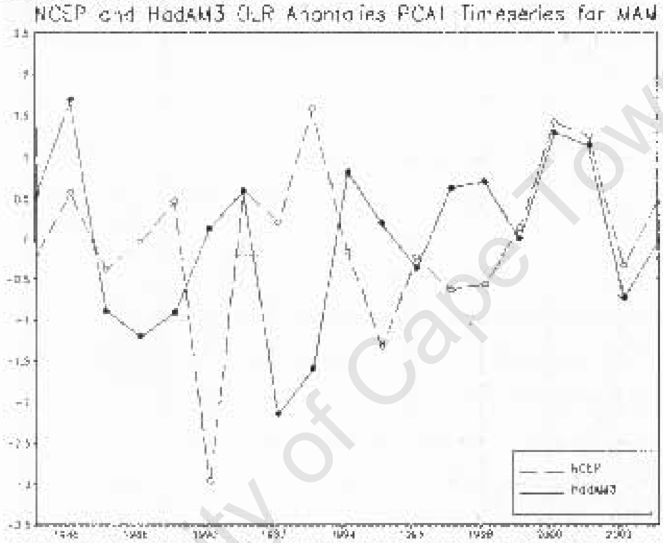

Fig. 23. Temporal patterns of NCEP and HadAM3 OLR anomalies first PCA for the MAM season

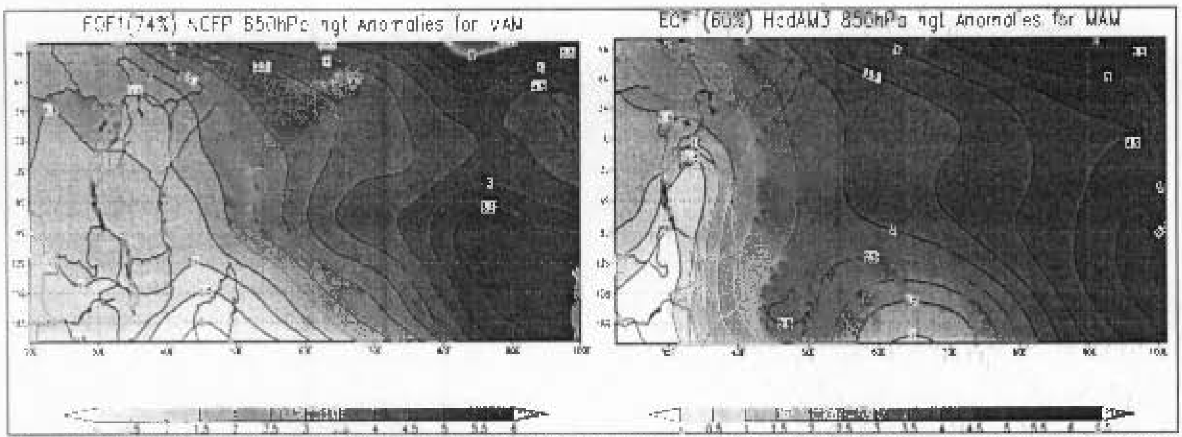

Fig. 24. The NCEP and HadAM3 model MAM 850hPa geopotential height anomalies first EOF with variance contribution of 74% and 60% respectively, positive EOF are shaded.

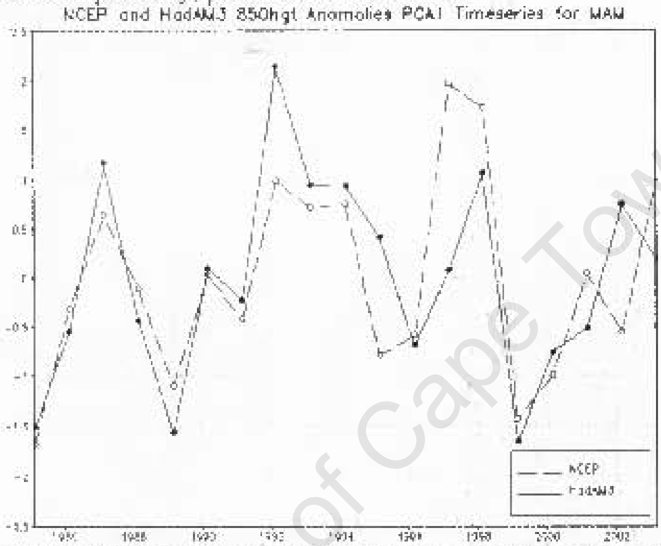

Fig. 25. Temporal patterns of NCEP and HadAM3 850hPa geopotential height anomalies first PCA for the MAM season

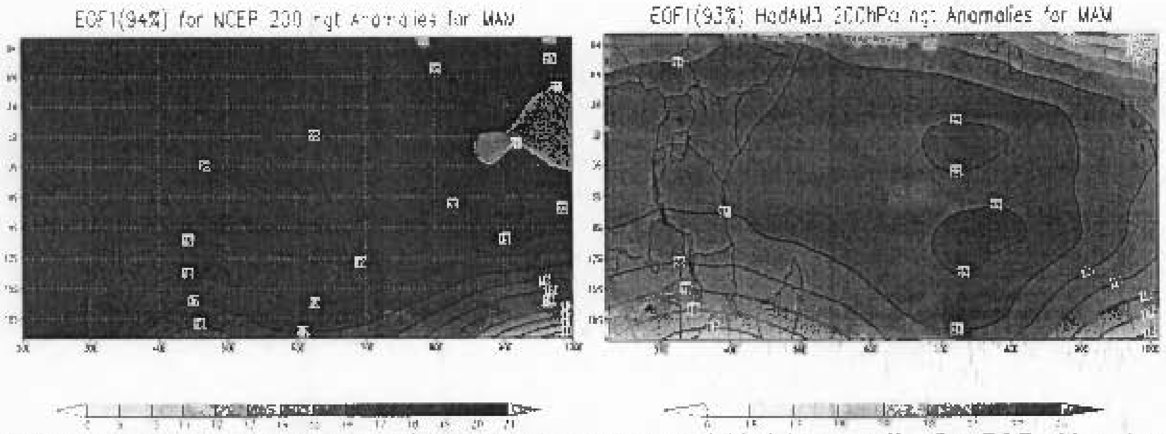

Fig. 26. The NCEP and HadAM3 model MAM 200hPa geopotential height anomalies first EOF with variance contribution of 94% and 93% respectively

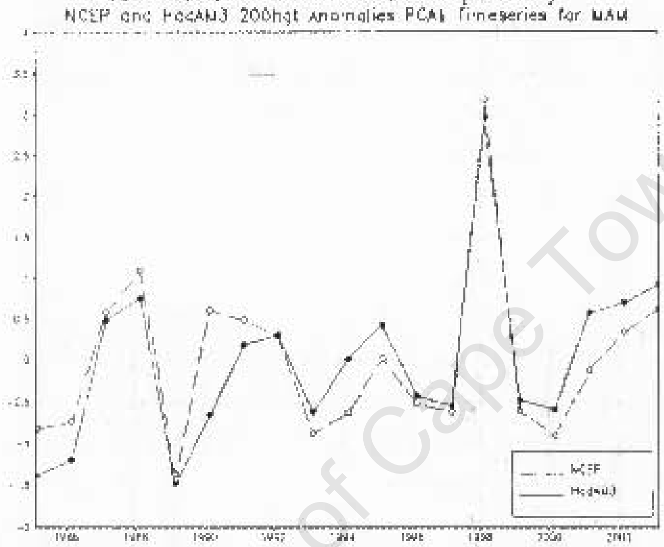

Fig. 27. Temporal patterns of NCEP and HadAM3 200hPa geopotential height anomalies first PCA for the MAM season.

4 Discussion

Previous work has indicated that Tanzanian rainfall has widespread spatial and temporal variability and this may largely be attributed to various factors that influence rainfall over the country at mesoscale, synoptic and large scales (Asnani, 1993).

Orography, inland water bodies and proximity to the ocean have been indicated as aspects that predominantly influence rainfall behaviour at a mesoscale level (Figs. 1-2). For example, longer seasons with more rainfall are experienced over areas influenced by these aspects than those that are not. Moisture influx from the ocean and lakes are largely attributed to high amounts of precipitation received over adjacent land areas. This can be observed over areas like Bukoba, Mwanza and Kigoma that are contiguous to Lake Victoria and Tanganyika. Enhanced convection over elevated terrain can significantly facilitate the formation of clouds that may precipitate over nearby land areas. Orographic rains are very common over the northern highlands of Arusha, Kilimanjaro and Tanga, the eastern arc highlands that pass through Morogoro and Iringa and the southern highlands of Mbeya and Ruvuma. Dodoma, Singida and Tabora are the only areas that may not be under a strong influence of orography, inland water bodies and proximity to ocean and consequently receive the shortest rainfall season and least amount of precipitation. This is in agreement with the remarks stipulated by Asnani (1993) that the ocean, inland lakes and orography influence Tanzanian rainfall variability significantly. It is therefore clear that the influence of the given aspects to rainfall variability over Tanzania cannot be overemphasized.

Delineation of seasons over the country is mainly attributed to the time when the ITCZ pass over different areas of the country. It influences the unimodal areas once a year and the bimodal areas twice due to the alignment of its zonal and meridional arm. The unimodal areas therefore experience extended and relatively uninterrupted rainfall between the end of October and the beginning of May while the bimodal areas experience rainfall that are interrupted between beginning of January and the beginning of March (Fig. 2).

ENSO is one major factor suggested as the cause for the interannual variability of Tanzanian rainfall during the OND season. Despite ENSO being strongly linked to Indian Ocean SSTAs, it does not have much impact on MAM seasonal rainfall which appears to be weakly forced by SSTAs only during March-April particularly over northern areas of East Africa (Camberlin and Philippon, 2002).

Wet OND seasons between 1985 and 2003 are 1986, 1989, 1997, 2000 and 2002; among them 1986, 1997 and 2002 were El Nino years while 2000 was a La Nina year (Fig. 4). The prominence of the 1997 El Nino was featured almost throughout the country and it is considered the strongest coupled El Nino/Indian Ocean Zonal Mode event in the last two decades (Yu and Reirecker, 1999; Webster et al., 1999). The El Nino impact over the Tanzanian coast was observed by Kijazi and Reason (2005) and shown that the impact is predominantly during the OND season and the northern coast is much more impacted than the southern coast. Other El Nino years during this period were 1991 and 1994 but their amount of rainfall is within the average range. Despite eight years (1987, 1993, 1995-1996, 1998-1999, 2001 and 2003) being observed as dry during OND, the only La Nina years found amongst them are 1995, 1998 and 1999. There were other La Nina years during this period but one of them showed near average rain (1988) and the other one was wet (2000). It is then noteworthy that during OND, most of the El Nino and La Nina years are wet and dry respectively.

Consistent with previous research which showed little ENSO impact on MAM rainfall, no obvious relationship was found in this study between the amount of rainfall and ENSO events. It may therefore be suggested that all the wet or dry MAM seasons during ENSO may have basically taken place by coincidence or influence of other atmospheric dynamics.

The comparison of GPCP/NCEP and HadAM3 model precipitation, OLR and geopotential height anomalies EOF and PCA revealed that their fields were much different between OND and MAM seasons. While the HadAM3 model ability in capturing the precipitation anomalies variability patterns shown in GPCP during OND was apparent, it was observed to be less comparable during MAM (Fig. 12-27). The HadAM3 model better performance in OND may be attributed to the fact that it is forced by observed SST which strongly influences the OND seasonal rains but has less influence on the MAM seasonal rains. It has been indicated that when the prevailing climatic systems are not strongly influenced by SST, it then becomes difficult for the models forced by SST to successfully present them

(Black, 2003). HadAM3 model, being forced by observed SST, may be less capable of presenting the climatic systems that are prevalent during the MAM season. In addition, the early Somali Jet and weak monsoon easterlies in HadAM3 are indicated as reducing rainfall over East Africa.

On the other hand, the relatively few observations over East Africa and the less accuracy of the satellite rainfall estimations may render the products derived from GPCP and NCEP less representative of real East African climatic conditions. In this regard, weather and climate systems prevailing over East Africa during MAM and OND in the GPCP or NCEP data may not be directly comparable to the observed conditions.

5 Conclusions and recommendations

The spatial and temporal scarcity of observed weather and climate data over Tanzania may be cited as one of the major limitations in weather and climate variability studies. Global atmospheric models and satellite derived data may be used as an alternative to observed data but the quality of such data is also questionable. However, they suffice to show general features of weather and climate variability at a synoptic scale. Regional atmospheric models may provide a substantially impetus in the better understanding of the spatiotemporal variability of Tanzanian climate and weather systems.

The success of HadAM3 model in capturing features of significance shown in GPCP precipitation data during the OND season may greatly be attributed to the fact that the SST anomalies which have a significance influence on the season are used to force the model. The HadAM3 model has therefore shown very little success in capturing features shown in GPCP precipitation data during the MAM season and this may be due to its weak monsoon easterlies and less influence of SST anomalies on the season in the real world. Investigations of the MAM season by using regional atmospheric models with improved monsoon winds which have a strong influence on the season as one of the boundary condition may be a more robust approach. Also, the assimilation more observed data into HadAM3 as they become available, may improve the ability of the model to represent climatic features more accurately.

References

Adler, R. F., G. J. Huffman and A. Chang, 2003: The Version-2 Global Precipitation Climatology Project (GPCP) monthly precipitation analysis (1979-present), *J. Hydrometeor.* 4 (6): 1147-1167

Alusa, A. L and M.T Mushi, 1974: A study of the onset, duration and cessation of the rains in East Africa. ***International Tropical Meteorological Meeting***, Nairobi, p 133–140.

Alusa, A. L. 1978: A note on the onset of the rains in East Africa. Kenya Meteorological Department (KMD), ***Research Report*** No 3 (78): 18p

Alusa, A. L and P.M Gwange, 1978: The occurrence of dry spells during the East Africa long rains. ***Research report*** 5/78, East African Institute for Meteorology, Nairobi, 1–18.

Amissah-Arthur A., S. Jagtap and C. Rosenzweig, 2002: Spatio-temporal effects of El Niño events on rainfall and maize yield in Kenya. ***Int. J. Climatol*** 22(15): 1849 - 1860

Anyah, R. O. and F. H. M. Semazzi, 2004: Simulation of the sensitivity of Lake Victoria basic climate to lake surface temperature. ***Theor. Appl. Climatol.*** 79: 55-69

Anyamba, E. K. and P. M. R. Kiangi, 1985: Mean motion field in East Africa at the level of the East African low level jet core. ***Meteorol. Atmos. Phys.*** 36(1): 29-41

Asnani, G. C. 1993: ***Tropical Meteorology***. Vol. 1, Indian Inst. Of Tropical Met, Pashan, India, 603pp

Beltrando, G. 1990: Space-Time Variability of Rainfall in April and October-November over East Africa during the Period 1932-1983. ***Int. J. Climatol.*** 10(7): 691-702.

Bergonzini, L., Y. Richard, L. Petit and P. Camberlin, 2004: Zonal circulations over the Indian and Pacific Oceans and the level of lakes Victoria and Tanganyika. ***Int. J. Climatol.*** 1613-1624.

Black, E. 2003: The Influence of Indian Ocean SST on tropical East Africa rainfall: Insights from observations and GCMs. ***UGAMP Newsletter.*** 27 6-8.

Camberlin, P. and N., Philippon, 2002: The East African March-May Rainy Season: Associated Atmospheric Dynamics and Predictability over the 1968-97 Period. ***J.***

Climate.15 (9): 1002-1019.

Camberlin, P. 1995. June–September rainfall in northeastern Africa and atmospheric signals over the tropics: A zonal perspective. ***Int. J. Climatol.*** 15: 773–783.

Chambers, D. P., B.D. Tapley and R. H. Stewart, 1999: Anomalous warming of the Indian Ocean coincident with El Niño. ***J. Geophy. Res***. 104: 3035-3047

Chen, M. and J.R. Bates, 1996: A comparison of climate simulations from a semi-Lagrangian and an Eularian GCM. ***J. Climatol***. 97: 1126-149

Cox, P. M., R. A. Bettes, C. B. Bunton, R. L. H. Essery, P. R. Rowntree and J. Smith, 1999: The impact of new land surface physics on the GCM simulation of climate and climate sensitivity. ***Climate Dynamics.*** 15: 183-203

Datta, R. R. 1981: Certain aspects of the monsoon precipitation dynamics over Lake Victoria. In: Lighthill, J. and R. P. Peace (eds). ***Monsoon dynamics***. Cambridge Univ. Press p 333-349

Dean S. M., B. N. Lawrence, R. G. Grainger and D. N. Heuff, 2005: Orographic cloud in a GCM: the missing cirrus. ***J. Climate Dyn***. 24: 771–780

Edwards, J.M. and A. Slingo, 1996: Studies with a flexible new radiation code I: choosing a configuration for a large-scale model. ***Q.J.R. Met. Soc***. 122: 689-719

Gregory, D., R. Kershaw and P. M. Inness, 1997: Parametrization of momentum transport by convection. II: tests in single-column and general circulations models. ***Q. J. R Met. Soc***. 123: 1153-1183.

Hastenrath, S. and L. Greischar, 1993: Further work on the prediction of Northern Brazil rainfall anomalies. ***J. Climate*** 6: 743-758.

Hastenrath, S. and Polzin D. 2004: Dynamics of surface wind field over the equatorial Indian Ocean. ***Q. J. R Met. Soc***. 130: 503–517.

Hutchinson, P. 1992: The Southern Oscillation and prediction of 'Der' season rainfall in Somalia. ***J. Climate***, 5: 525–531.

Indeje, M., and F. H. M Semazzi, 2000: Relationship between QBO in the lower equatorial stratospheric zonal winds and East Africa seasonal rainfall ***Meteorol. Atmos. Phys.*** 73: 227-244.

Indeje, M., F. H. M, Semazzi and L. A. Ogallo, 2000: ENSO signals in East Africa rainfall seasons. ***Int. J. Climatol.*** 20: 19-40

Janowiak, J. E. 1988: An investigation of interannual rainfall variability in Africa. ***J. Climate***. 3: 240-255

Josey, S. A. 1999: Seasonal to interannual variability in the SOC air-sea flux dataset and Hadley Centre Atmospheric Model Version 3. ***Southampton Oceanographic Centre Internal Document No. 51.***

Kabanda, T. A and M. R. Jury, 1999: Interannual variability of short rains over northern Tanzania. ***J. Clim Res*** 13:231-241

Kabanda, T. A and M. R. Jury, 2000: Synoptic evolution of composite wet spells over northern Tanzania. ***J. Clim Res*** 15:239-248

Kalnay E, and Co-authors, 1996: The NCEP/NCAR 40-year Reanalysis Project. ***Bull Amer. Meteor Soc*** 77: 437–471

Kijazi, A.L and C.J.C. Reason, 2005: Relationships between intraseasonal rainfall variability of coastal Tanzania and ENSO. ***J. Theor. And Appl. Climatology*** 82(3-4): 153-176

Lau, K. and P. J. Sheu, 1988: Annual cycle, Quasi-Biennial Oscillation and Southern Oscillation in global precipitation. ***J. Geophy. Res.*** 93(D9): 10975-10988.

Mapande, A. T and C. J. C. Reason, 2005: Links between rainfall variability on intraseasonal and Interannual scales over western Tanzania and regional circulations and SST patterns. ***J. Meteor. and Atmos. Physics*** 89:215-234.

Mhita, M. S. 2003: ***Development of new seasonal climate prediction tools through analysis of onset and cessation of seasonal rains associated with El Niño/La Niña events***: The report for the pilot applications project. TMA, Dar es Salaam, Tanzania

Mhita, M.S and I.R Nassib 1987: The onset and end of rain in Tanzania. Proc 1st Tech Conf Meteorol Res East South Afr, Nairobi, p 101–115.

Mistry, V. and Conway, D.2003: Climatological factors responsible for variations in levels of Lake Victoria. ***Int. J. Climatol*** 23: 67-89.

Mitchell, T. D. and D. J. Philip, 2005: An improved method of constructing a database of monthly climate observations and associated high-resolution grids. ***Int. J. Climatol.*** 25: 693–712

Mpeta, E. J. 1997. ***Intra-seasonal convection dynamics over southwest and northeastTanzania: an observational study***. M.Sc. dissertation: University of Cape Town.

Mukabana, J. R and R. A. Pielke, 1996: Investigating the influence of synoptic scale winds and meso-scale circulations and diurnal weather patterns over Kenya using a mesoscale numerical model. ***Mon. Wea. Rev.*** 124: 224-243

Murtugudde, R., J. P. McCreary and A.J. Buchalacchi, 2000: Oceanic processes associated with anomalous events in the Indian Ocean with relevance to 1997-98. ***J.Geophy. Res***. 105: 3295-3306.

Mutai, C. C. and M. N. Ward, 1998: ***Predictability East Africa short rains on intraseasonal to interannual timescales***. Proc. 23rd Annual Climate Diagnostic Workshop, Miami, Florida October 26-30. NOAA, Washington, DC.

Mutai, C.C. and M.N. Ward, 2000: East African Rainfall and the Tropical Circulation/Convection at Interannual and Intraseasonal Timescales. ***J. Climate***. 13: 3915-3939.

Nicholson, S. E and D. Entekhabi, 1986: The quasi-periodic behaviour of rainfall variability in Africa and its relationship to the Southern Oscillation. ***Arch. Met. Geoph. Biol.***, Ser. A, 34: 311

Nicholson, S. E., 1996: A review of climate dynamics and climate variability in eastern Africa. In: Odada, E. and Johnson, T. C (eds). ***The Limnology climatology and paleoclimatology of East Africa Lakes***. New York, Gordon and Breach 57pp.

Nicholson, S. E. and J Kim, 1997: The Relationship of the El Niño–Southern Oscillation to African Rainfall ***Int. J. Climatol.*** 17: 117–135

Nicholson, S. E. 1999: Historical and Modern Fluctuations of Lakes Tanganyika and Rukwa and Their Relationship to Rainfall Variability. ***J. Climatic Change.*** 41(1): 53-71

Nyenzi, B. S. 1988: ***Mechanisms of East Africa rainfall variability***. PhD. Thesis, Florida State University

Ogallo L. J. 1988: Relationship between seasonal rainfall in East Africa and Southern Oscillation. ***Int. J. Climatol*** 8: 34-43

Ogallo L. J. 1989: The spatial and temporal patterns of the East Africa seasonal rainfall derived from PCA. ***Q. J. Roy Met. Soc***. P 145-167

Ogallo, L. J. and Suleiman K. A. 1988: ***Rainfall characteristic in East Africa and during the El Niño year***. Proc 1st Tech Conf Meteor Res East South Africa, Nairobi, p76-80

Ogallo, L. J., 1982: Quasi-periodic patterns in the East African rainfall record. ***Kenya J. Sci. and Techn.*** A3: 43-54

Ogallo, L. J., J. E. Janowiak and M. S. Halpert 1988: Teleconnections between seasonal rainfall over East Africa and global sea surface temperature anomalies. ***J Met. Soc Jpn*** 66(6): 807-821

Okoola, R. E. 1999: A diagnostic study of the eastern Africa monsoon circulation during the northern hemisphere spring season. ***Int. J. Climatol*** 19: 143-168.

Podsetchine, V., T. Huttula and H. Savijärvi, 1999: A three dimensional-circulation model of Lake Tanganyika. ***J. Hydrobiologia.*** 407(0): 25-35.

Pope, V. D., M. Gallani, P. Rowntree, and R. Stratton, 2000: The impact of new physical parametrizations in the Hadley Centre climate model: HadAM3. ***J. Climate Dyn.***, 16:123–146.

Reason C. J. C, R. J. Allan, J. A. Lindesay and T. J. Ansell, 2000: ENSO and Climatic Signals across the Indian Ocean Basin in the global context: Part I, Interannual Composite patterns. ***Int. J. Climatol.*** 20: 1285–1327

Reason, C. J. C. and D. Jagadheesha, 2005: A model investigation of recent ENSO impacts over southern Africa. ***Meteorol Atmos Phys 89***, 181–205

Rodhe, H. and H. Virji, 1976: Trends and periodicity in East African rainfall. ***Mon. Wea. Rev.*** 104: 307-315

Ropelewski, C.P. and M.S. Halpert, 1987: Global and regional scale precipitation patterns associated with El Niño/Southern Oscillation. ***Mon. Wea. Rev.*** 115: 1606-1626.

Saji. N. H., B.N. Goswami, P. N. Vinayachandran and T. Yamagata, 1999: A dipole in the tropical Indian Ocean. ***Nature.*** 401: 360-363.

Sun, L., F. H. M. Semazzi, F. Giorgi and L. A. Ogallo, 1999(a): Application of the NCAR Regional Climate Model to Eastern Africa; Part I: Simulation of the short rains of 1988. ***J. Geophy. Res.*** 104: 6529-6548.

Sun, L., F. H. M. Semazzi, F. Giorgi and L. A. Ogallo, 1999(b): Application of the NCAR Regional Climate Model to Eastern Africa; Part II: Simulation of interannual variability of short rains. ***J. Geophy. Res.*** 104: 6549-6562

Toure, Y. M. and W. B. White, 1997: Evolution of ENSO signals over the indo-pacific domain. ***J. Physical Oceanography***. 27: 683-696.

Webster, P. J., J. P. Loschnigg and R. R. Leben, 1999: Coupled ocean-atmosphere dynamics in the Indian Ocean during 1997-98, ***Nature***. 401: 356-359

Williamson, D. L., J. G. Olsen and B. A. Boville, 1998: A comparison of semi-Lagrangian and Eulerian tropical climate simulations. ***Mon Weather Rev***. 126: 991-1000

Yu, L. and M. M. Reinecker, 1999: Mechanisms for the Indian Ocean warming during 1997-98 El Niño. ***Geophy. Res. Letters***. 26: 735-738.

Appendix: Second and third EOF/PCA figures

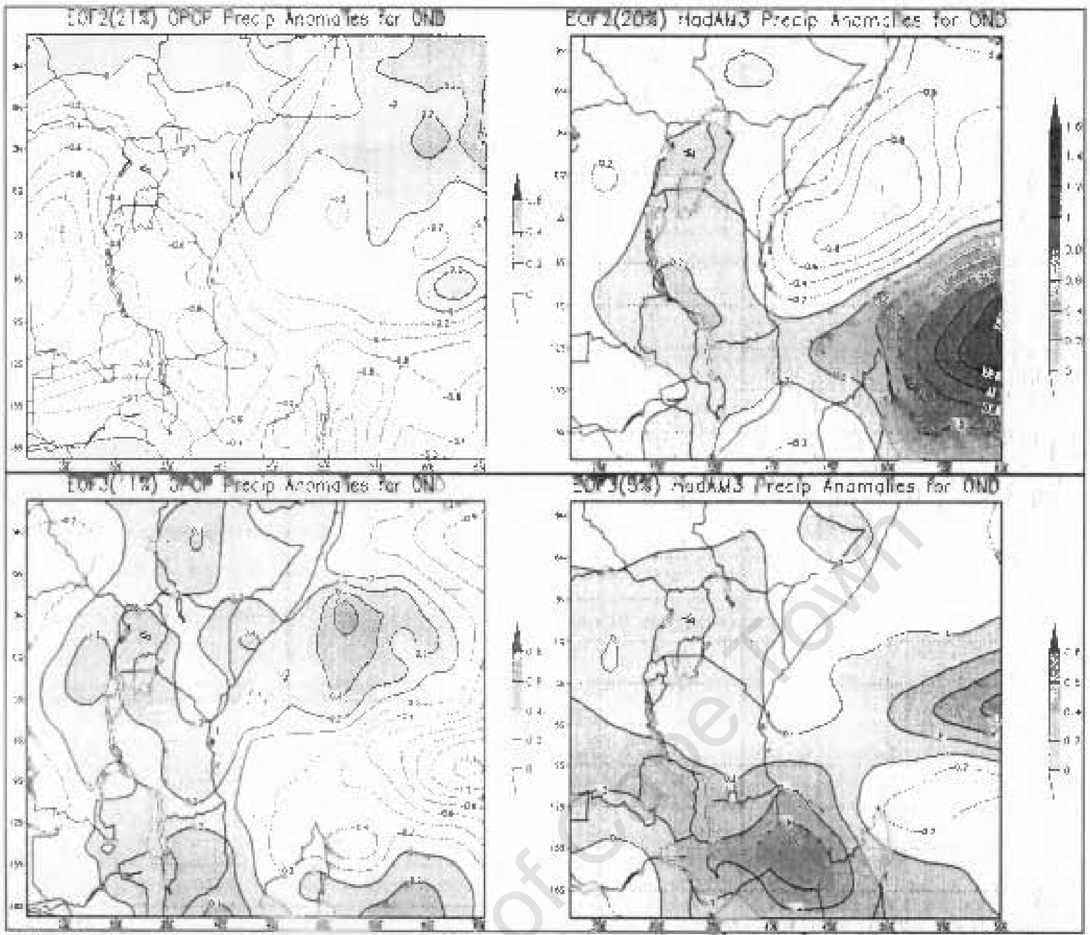

The GPCP and HadAM3 OND season precipitation anomalies 2nd and 3rd EOFs, the positive EOFs are shaded.

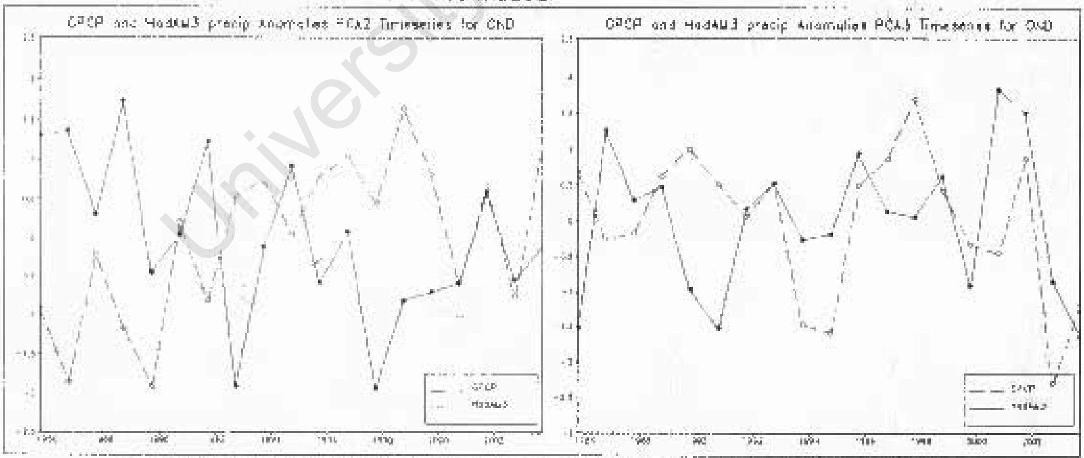

The GPCP and HadAM3 OND season precipitation anomalies 2nd and 3rd PCAs

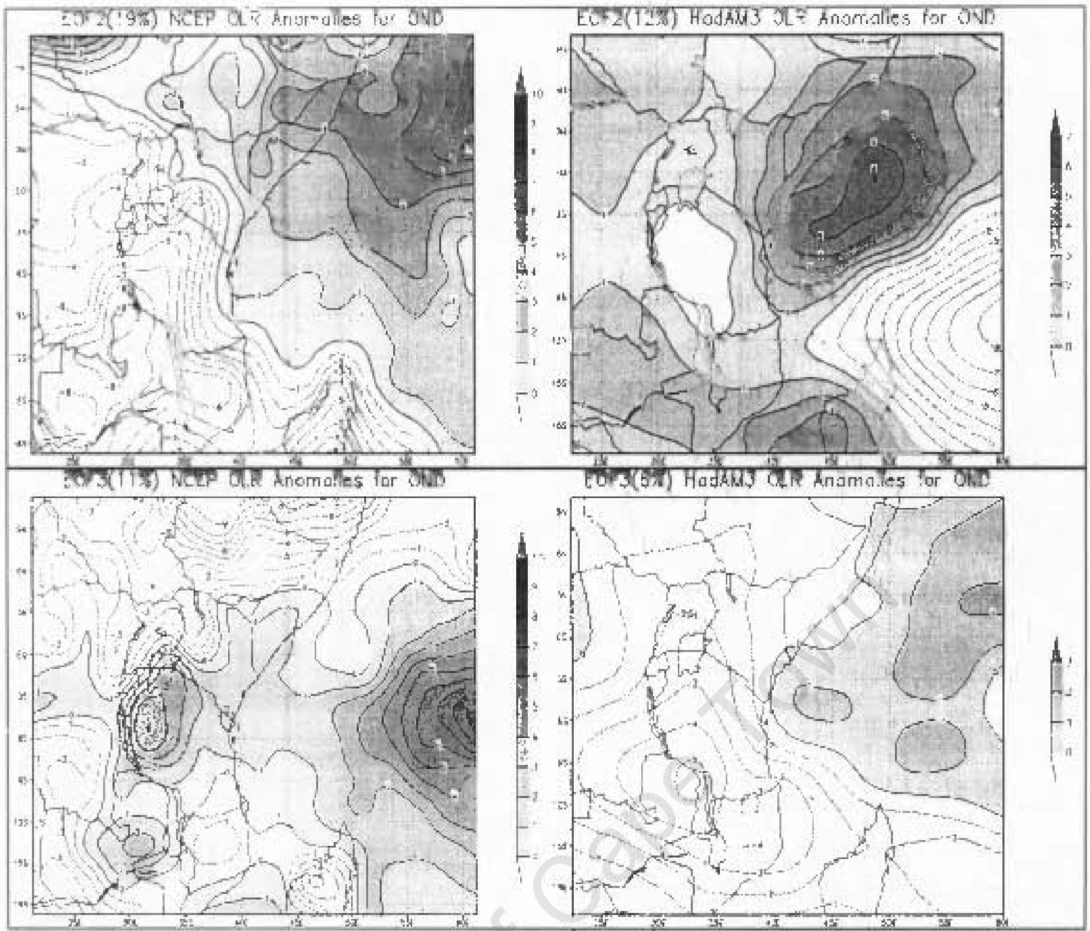

The NCEP and HadAM3 OND season OLR anomalies 2[nd] and 3[rd] EOFs, the positive EOFs are shaded

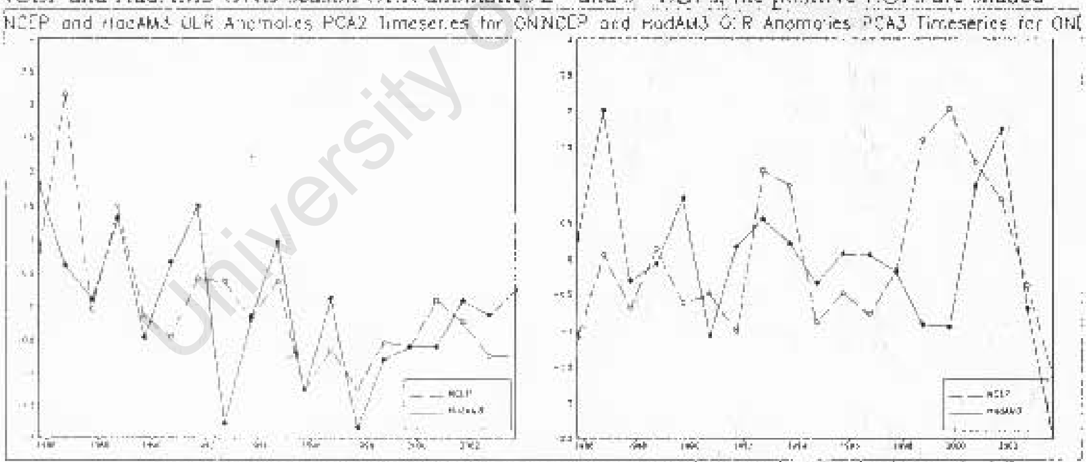

The NCEP and HadAM3 OND season OLR anomalies 2[nd] and 3[rd] PCAs

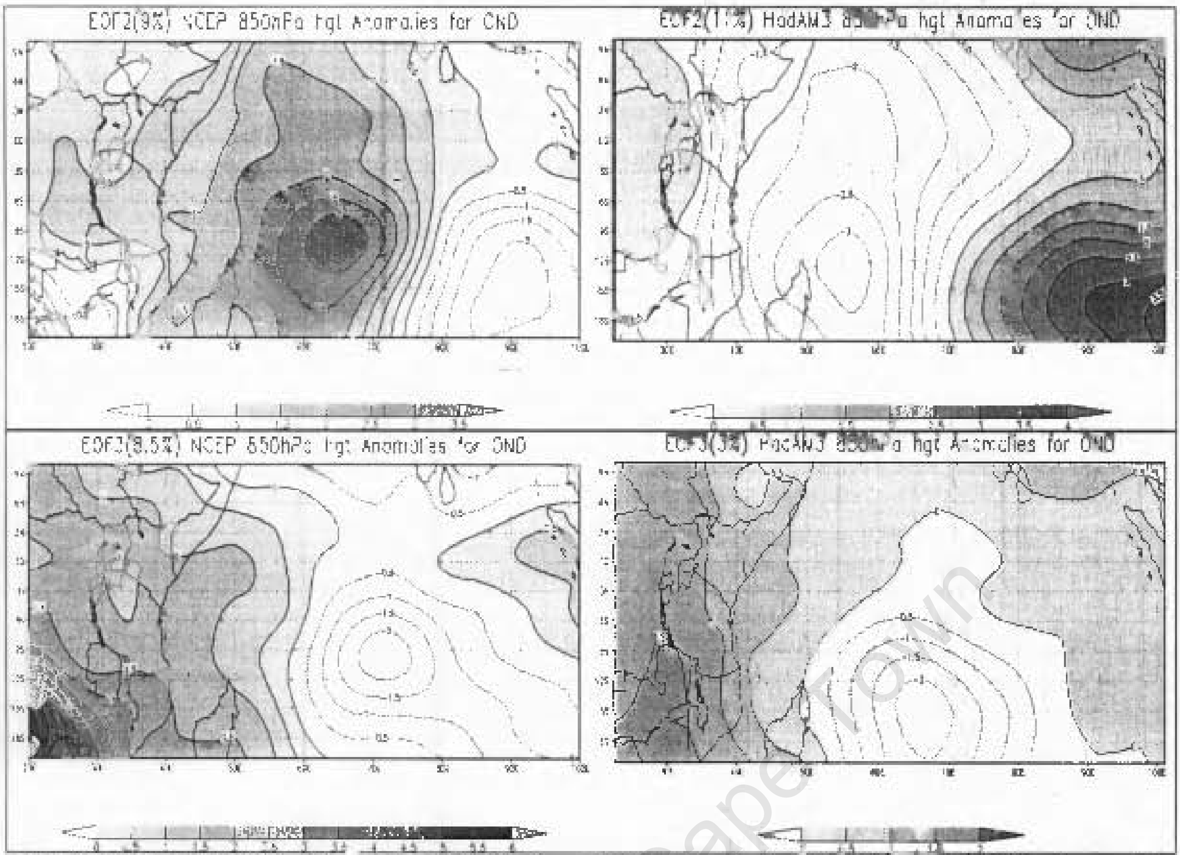

The NCEP and HadAM3 OND season 850hPa Geopotential height anomalies 2nd and 3rd EOFs, the positive EOFs are shaded

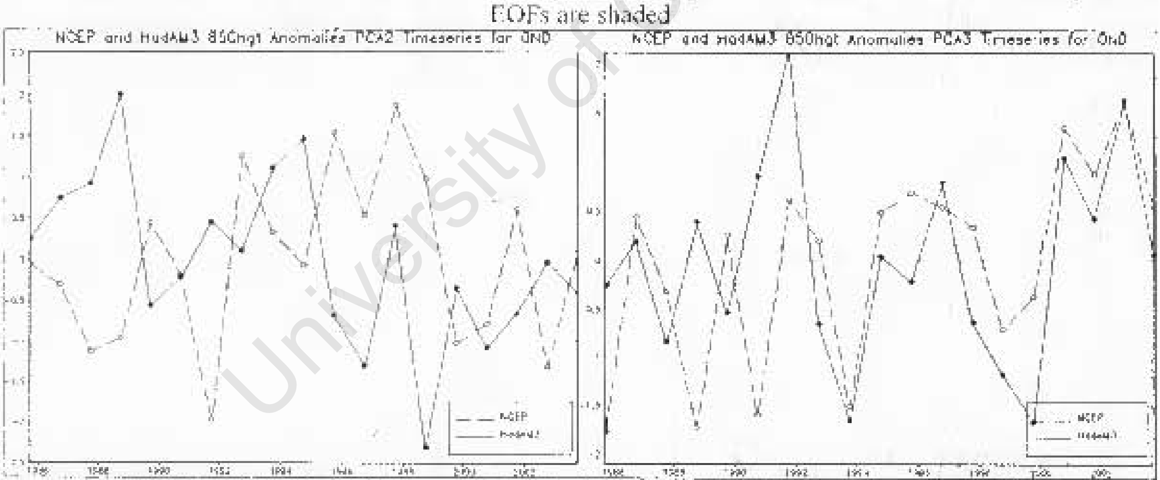

The NCEP and HadAM3 OND season 850hPa Geopotential height anomalies 2nd and 3rd PCAs

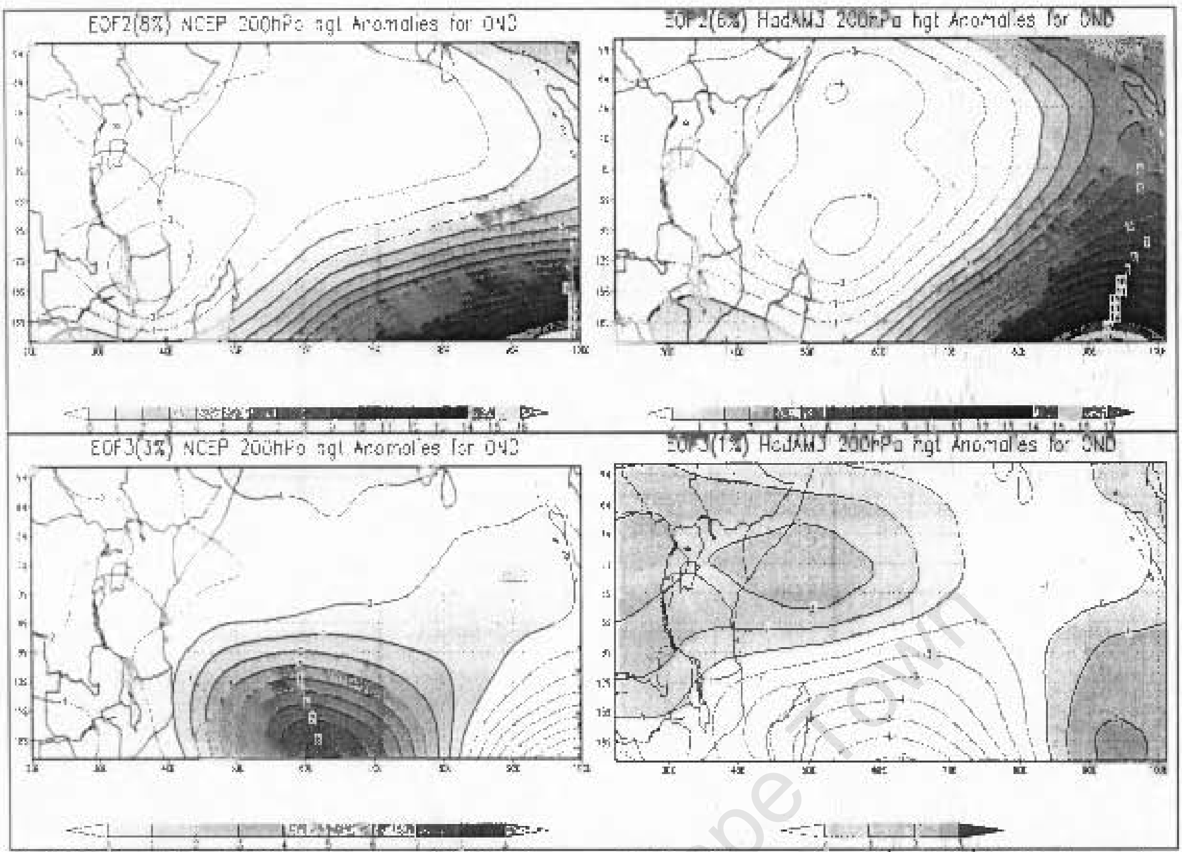

The NCEP and HadAM3 OND season 200hPa Geopotential height anomalies 2nd and 3rd EOFs, the positive EOFs are shaded

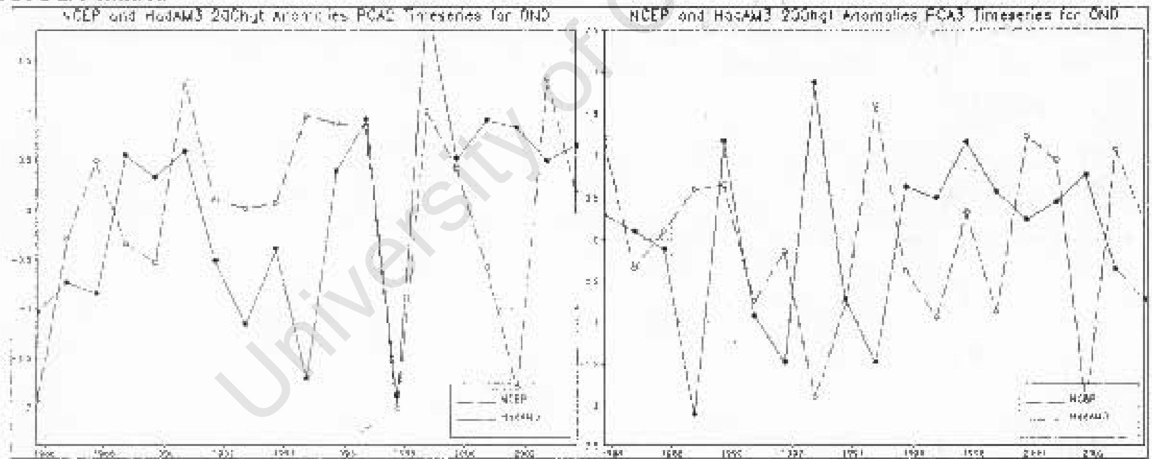

The NCEP and HadAM3 OND season 200hPa Geopotential height anomalies 2nd and 3rd PCAs

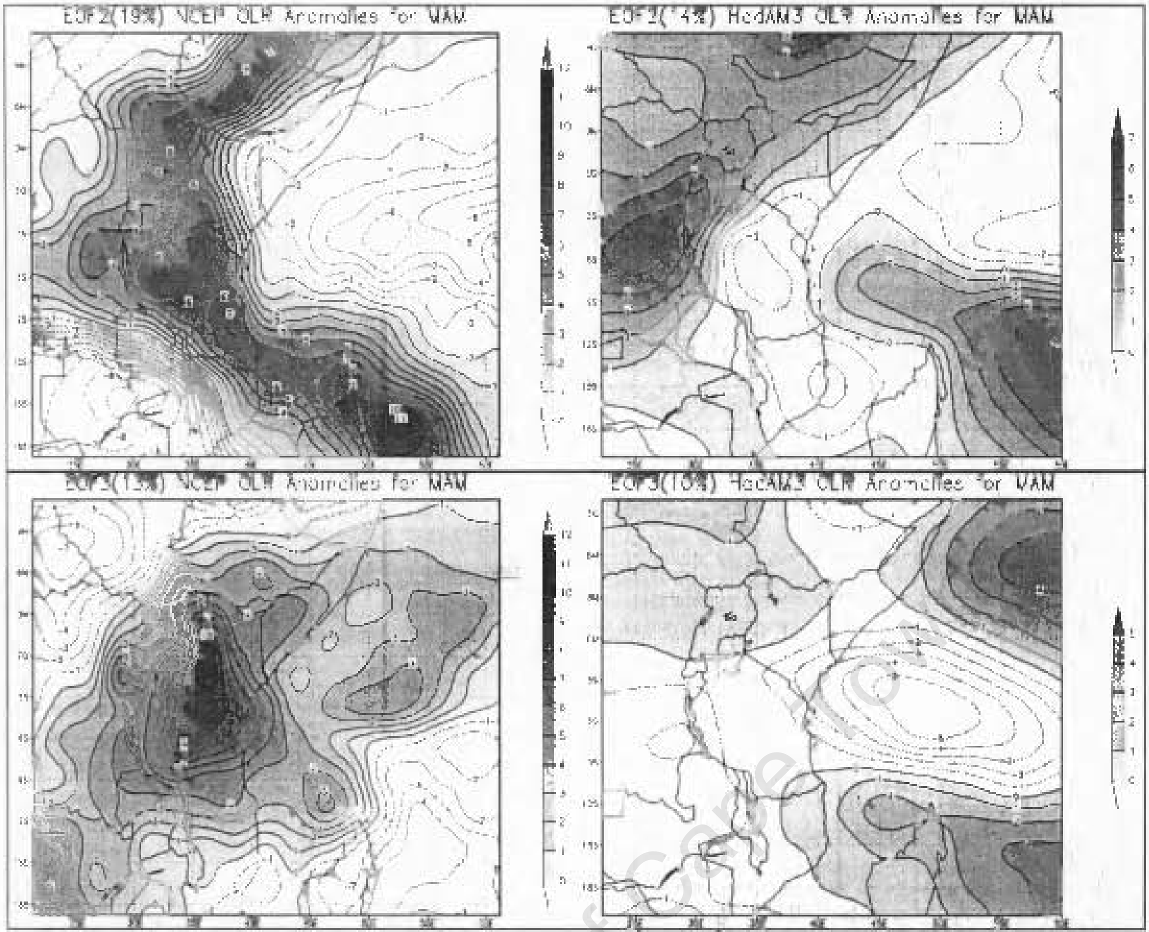

The NCEP and HadAM3 MAM season OLR anomalies 2nd and 3rd EOFs, the positive EOFs are shaded

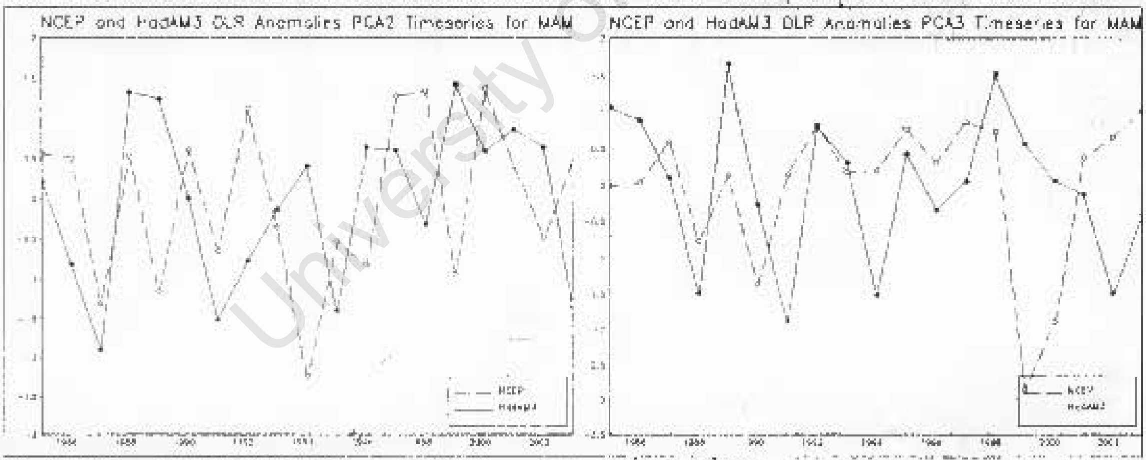

The NCEP and HadAM3 MAM season OLR anomalies 2nd and 3rd PCAs

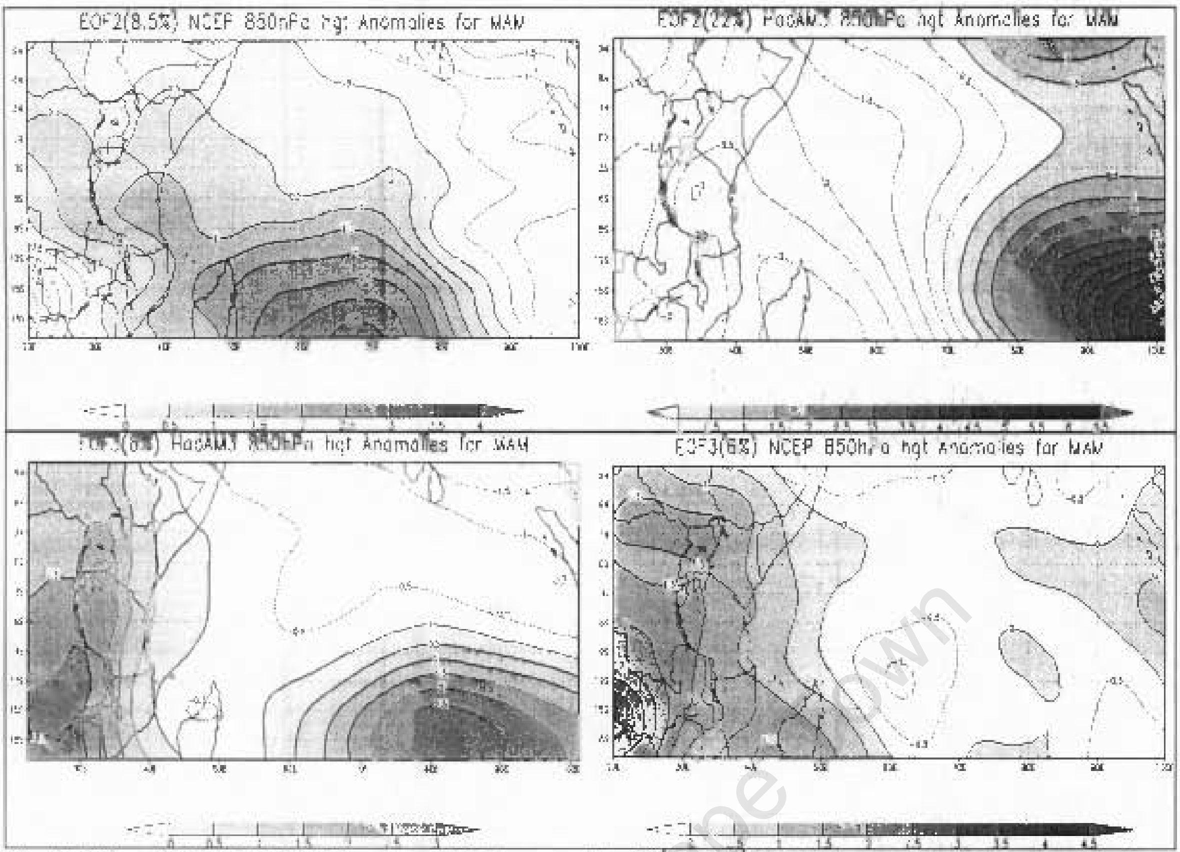

The NCEP and HadAM3 MAM season 850hPa anomalies 2nd and 3rd EOFs, the positive EOFs are shaded

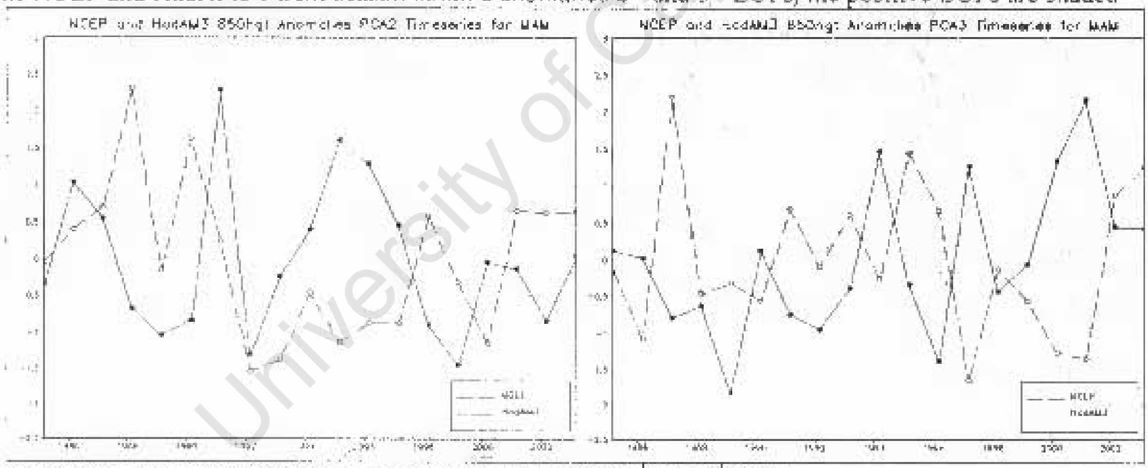

The NCEP and HadAM3 MAM season 850hPa anomalies 2nd and 3rd PCAs

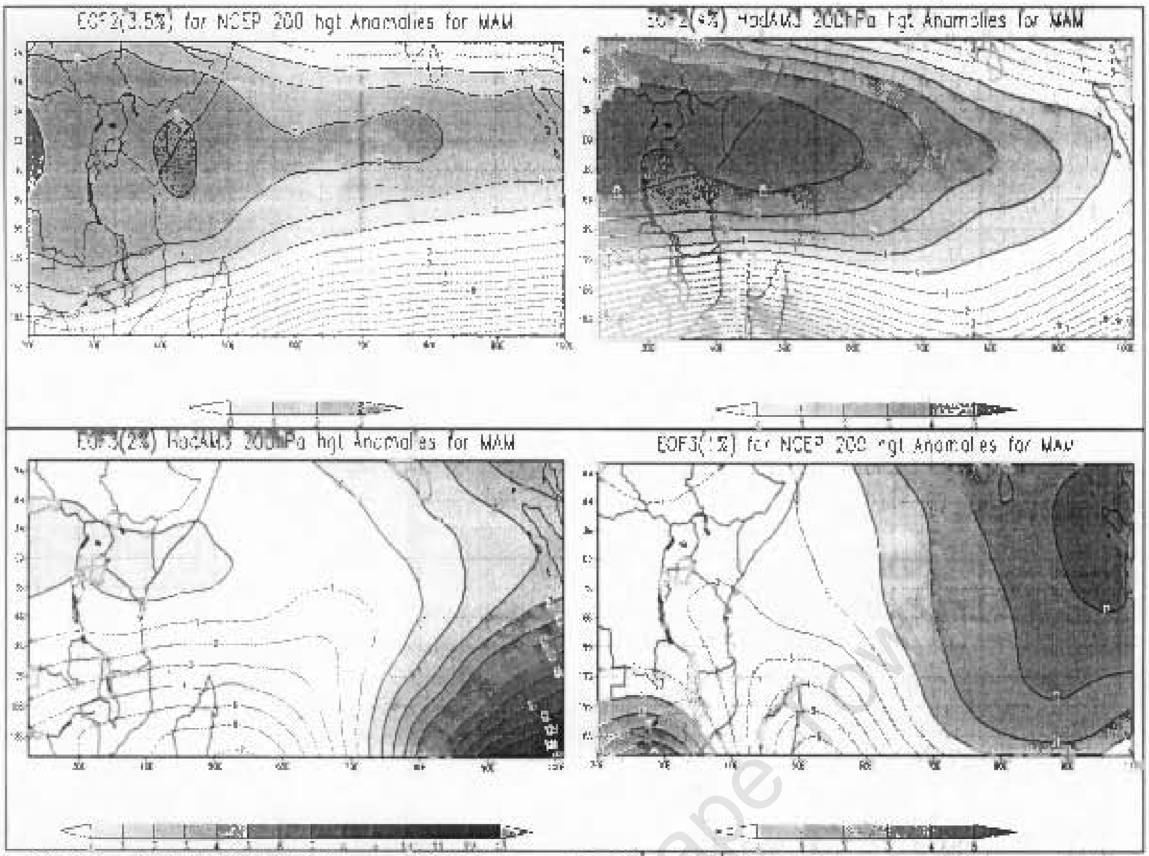

The NCEP and HadAM3 MAM season 200hPa anomalies 2nd and 3rd EOFs, the positive EOFs are shaded

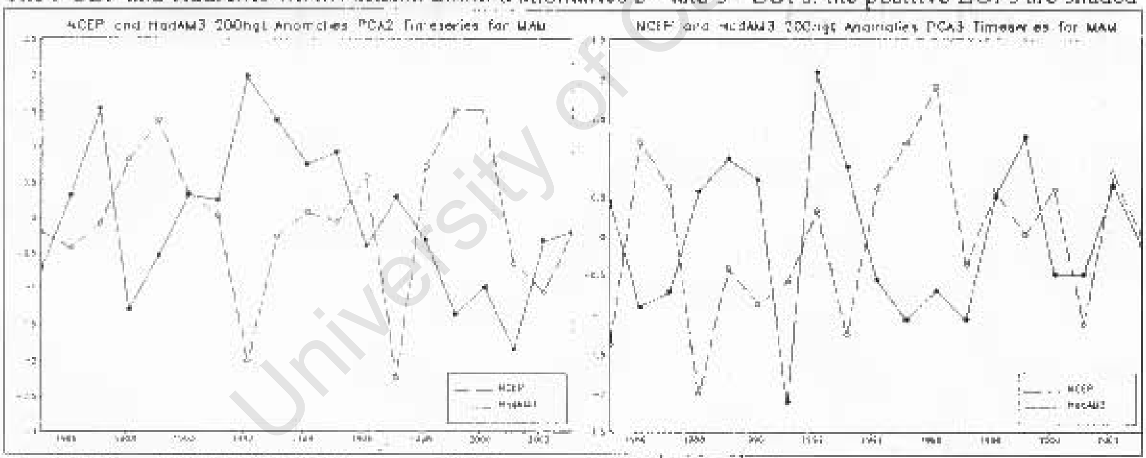

The NCEP and HadAM3 MAM season 200hPa anomalies 2nd and 3rd PCAs